Rate Independent Crystal Plasticity

by

Manish Kothari

B.Tech. in Mechanical Engineering,
Indian Institute of Technology, Madras, 1992

Submitted to the Department of Mechanical Engineering
in partial fulfillment of the requirements for the degree of

Master of Science in Mechanical Engineering

at the

MASSACHUSETTS INSTITUTE OF TECHNOLOGY

June 1995

Author .....
Department of Mechanical Engineering
May 12, 1995

Certified by .....
Dr. Lallit Anand
Professor
Thesis Supervisor

Accepted by .....
Ain A. Sonin
Chairman, Departmental Committee on Graduate Students

Rate Independent Crystal Plasticity

by

Manish Kothari

B.Tech. in Mechanical Engineering,

Indian Institute of Technology, Madras, 1992

Submitted to the Department of Mechanical Engineering
on May 12, 1995, in partial fulfillment of the
requirements for the degree of

Master of Science in Mechanical Engineering

Abstract

The problem of non-uniqueness in the selection and determination of the amount of shear on the active slip systems has plagued the rate-independent crystal plasticity theories for several years. A new large deformation rate-independent crystal plasticity theory is fromulated which overcomes this long standing problem. The model has been implemented in a commerical finite element program ABAQUS/Implicit and ABAQUS/Explicit. The accuracy of the model has been evaluated by comparing the results for simple tensile deformation on f.c.c single crystals and a simple compression experiment on polycrystalline OFHC copper against the results of the rate-dependent model of Kalidindi, Bronkhorst and Anand (1992) in the rate-independent limit. Our calculations show that the results from the rate-independent model are in excellent aggreement with those of the rate-dependent model in the rate-independent limit.

Thesis Supervisor: Dr. Lallit Anand
Title: Professor

Acknowledgments

I would like to express my sincere thanks to all those people, whose input and advice over the past three years has been invaluable. First and foremost, I am indebted to my advisor and mentor, Prof. Anand, for his guidance, patience, encouragement and financial support without which this work would not have been possible. I owe all my confidence and the ability in dealing with problems, not just in research, to him. I am very grateful to him for that. He has helped me lay a foundation on which I hope to complete my ph.d and build a successful career. I would also like to thank him for letting me incorporate parts of his paper into my thesis.

I would like to thank Christine Allan, my mentor in experimental work, for her invaluable help and guidance. I am very grateful to my colleagues Fred Haubensak, Srihari, Chuang Chia, Brian, Ganti, Clarence, Omar, Apostollos, Jian and John for the fruitful discussions on research as well as on other "issues". I have learnt a lot from them and significantly improved my experimental and computational skills.

Thanks to my parents, my brother and my sister who have always been a source of inspiration and support during difficult times.

Contents

List of Figures

List of Tables

Chapter 1

Introduction

The quantitative description of plastic flow by crystallographic slip may be traced back to the early work of Taylor and Elam (1923, 1925), and Taylor (1938a, 1938b). Constitutive equations for elastoplastic behavior of ductile single crystals from the standpoint of modern continuum mechanics were first formulated by Mandel (1965) and Hill (1966), and extended to finite deformations by Rice (1971), Hill and Rice (1972), Asaro and Rice (1977), and Asaro (1983a,b). For a recent review see Havner (1992). In these models, intended for low homologous temperatures, the plastic deformation of single crystals by crystallographic slip is idealized to be *rate-independent*.

There have been three long-standing problems in the rate-independent theory of crystal plasticity. The first is to determine which slip systems are active, and the second is to determine the increments of shear on the active slip systems. Third, because of the typical multiplicity of slip systems in ductile crystals, the selection of slip systems required to produce an arbitrary deformation increment is not necessarily unique. These features of the rate-independent theory of plasticity pose a problem when the constitutive theory is applied to the numerical solution of boundary value problems. The first numerical calculations for a two-dimensional boundary value problem for non-homogeneously deforming rate-independent elastic-plastic single crystal, whose geometry was idealized in terms of a planar double slip model, are those of Peirce *et al.* (1982). Because of a lack of a robust solution strategy to determine the active slip systems and the amount of slip on these systems, the element stiffness matrices in the the finite element scheme of Pierce *et al.* became singular for a particular choice of a slip system hardening rule, and their numerical scheme broke

down.

To overcome the limitations of crystal plasticity models based on a rate insensitive idealization of crystalline slip, Asaro and Needleman (1985) developed a simple *rate-dependent* crystal plasticity model, which uniquely predicts constitutive response for arbitrary deformation histories. Specifically, Asaro and Needleman (1985) proposed that the shearing rate $\dot{\gamma}^\alpha$ on a slip system α is uniquely specified by

$$\dot{\gamma}^\alpha = \dot{\gamma}_0 \left| \frac{\tau^\alpha}{s^\alpha} \right|^{(1/m)} \operatorname{sign}(\tau^\alpha) . \tag{1.1}$$

In the equation above, τ^α is the resolved shear stress on the slip system, and $s^\alpha (> 0)$ is the slip system deformation resistance. The parameter $\dot{\gamma}_0$ is a reference rate of shearing, and the parameter m characterizes the material rate sensitivity. The rate independent limit is $m \to 0$. The slip system shear rate is uniquely specified by this equation, and is nonvanishing as long as the resolved shear stress τ^α on that system is not identically zero.

In crystal plasticity theories the slip system resistance parameters s^α are taken to evolve according to

$$\dot{s}^\alpha = \sum_\beta h^{\alpha\beta} \left| \dot{\gamma}^\beta \right| ,$$

where $\dot{\gamma}^\beta$ is the shearing rate on slip system β, and the matrix $\left[h^{\alpha\beta} \right]$ describes the rate of increase of the deformation resistance on slip system α due to shearing on slip system β; it describes both self hardening and latent hardening of the slip systems. The use of the absolute value of $\dot{\gamma}^\beta$ in the hardening equation reflects the assumption that the hardening behavior is not significantly affected by the direction of shearing on a slip system. Each element $h^{\alpha\beta}$ depends on the deformation history. It is fair to state that at present these instantaneous hardening moduli $h^{\alpha\beta}$ are the least well characterized part of the constitutive equations for crystal elastoplasticity[1].

In the rate-dependent formulation of Asaro and Needleman (1985), there is no division of slip systems into "active" or "inactive" sets; instead all slip systems always slip at a rate which depends on the current stress and slip system deformation resistance. Thus once the stress state is known (which is in their formulation), then the slipping rates on all possible slip systems are uniquely determined; and in this, no restrictions on the form of

[1] In an f.c.c crystal there are 144 elements that need to be specified.

the hardening matrix $\left[h^{\alpha\beta}\right]$ are required[2].

Although there has been considerable recent progress that has been made in the extension and application of the rate-dependent crystal plasticity model of Asaro and Needleman (1985) to the solution of important boundary value problems (c.f., e.g., Kalidindi *et al.*, 1992; Bronkhorst *et al.*, 1992; Anand and Kalidindi, 1994), it is still of substantial technical interest to develop a robust calculation scheme to determine the active slip systems and the corresponding shear increments for the *rate-independent* theory of crystal plasticity, for physically realistic, but essentially arbitrary hardening matrices $\left[h^{\alpha\beta}\right]$. The purpose of this paper is to present such a scheme.

In Section 2 we formulate a rate-independent constitutive model of crystal plasticity. In Chapter 3 we develop a similar *incremental formulation* for the model which is suitable for direct numerical implementation in displacement based finite element programs, and briefly describe the details of our numerical implementation of the constitutive model in a finite element program. In Chapter 4 we show results of the calculation of stress-strain curves, slip system activity, and evolution of crystal lattice orientation for tension tests on crystals initially oriented for single-slip and multi-slip for both non-hardening, $h^{\alpha\beta} = 0$, and a simple hardening rule and a simple compression simulation on a polycrystalline OFHC copper at a compressive strain of 100/In order to obtain a tractable description of crystal hardening, several simple forms for the hardening matrix have been proposed in the past, and these have been reviewed by Peirce *et al.* (1982), and more recently by Havner (1992), and Bassani (1994). In their numerical calculations Peirce *et al.* (1982) used the following simple form for the hardening moduli:

$$h^{\alpha\beta} = qh + (1-q)h\delta^{\alpha\beta},$$

with h denoting the self hardening rate and the parameter q with values in the range, $1 < q < 1.4$, representing a latent hardening parameter. The latent hardening parameter q is not necessarily a constant, and may of course be history dependent just as the self

[2]There has been a long history of considerations of possible mathematical restrictions on the hardening matrix $\left[h^{\alpha\beta}\right]$ in order to formulate a complete theory of *rate-independent* crystal plasticity. Early in the development of the theory, Hill (1966) noted that with finite strain effects neglected (see Chapter 2 for a more complete discussion), positive definiteness of the hardening matrix was a sufficient condition to ensure unique slipping rates. Experiments on the other hand suggest that latent hardening rates are generally somewhat larger than the self hardening rates which means that the matrix $\left[h^{\alpha\beta}\right]$ may be indefinite. As noted earlier, at present the instantanteous hardening moduli $\left[h^{\alpha\beta}\right]$ are not well characterized.

hardening parameter h is. This simple form for $h^{\alpha\beta}$ yields an acceptable description of the physical phenomena of latent hardening[3]. We present our calculations for $q = 1.4$, which is in the range of values of q for which the calculation procedures of Peirce *et al.* (1982) broke down. In 1982 Peirce *et al.* conjectured that, "It may well be that no unique description of of texture development, and therefore of polycrystalline behavior at finite strains, is possible within a rate-independent idealization, at least within one that attempts to describe latent hardening in a realistic way." We shall show that our new formulation and calculation procedure for rate-independent plasticity overcomes this long-standing conjectured limitation of the rate-independent theory. Indeed, we shall show by comparing the predictions from our computational procedure for the rate-independent theory against corresponding predictions from a procedure for the rate-dependent theory (Kaldindi *et al.*, 1992) for a low value of the rate sensitivity parameter m, that the results from the two procedures are essentially indistinguishable.

[3]However, see the recent papers by Wu *et al.* (1991) and Bassani *et al.* (1991) for some recent work on latent hardening in single crystals.

Chapter 2

Constitutive Model

We shall use notation which is now common in modern continuum mechanics (e.g. Gurtin, 1981). In particular, the inner product of two vectors $\mathbf{u}$ and $\mathbf{v}$ will be denoted by $\mathbf{u} \cdot \mathbf{v}$. The tensor product of two vectors $\mathbf{u}$ and $\mathbf{v}$ will be denoted by $\mathbf{u} \otimes \mathbf{v}$; it is the tensor which assigns to each vector $\mathbf{w}$ the vector $(\mathbf{v} \cdot \mathbf{w})\, \mathbf{u}$. The symmetric and skew parts of a second rank tensor $\mathbf{S}$ are denoted by $\text{sym}\mathbf{S} = (1/2)(\mathbf{S}+\mathbf{S}^T)$ and $\text{skw}\mathbf{S} = (1/2)(\mathbf{S}-\mathbf{S}^T)$, respectively. The inner product of two tensors $\mathbf{S}$ and $\mathbf{T}$ is defined by $\mathbf{S} \cdot \mathbf{T} = \text{trace}\left(\mathbf{S}^T\mathbf{T}\right)$.

At each time, the variables governing the response of our isothermal constitutive model are: (*i*) The velocity gradient, $\mathbf{L}$. (*ii*) The Cauchy stress, $\mathbf{T}$. (*iii*) Crystal slip systems, labeled by integers α. Each slip system is specified by a unit normal $\mathbf{n}^\alpha$ to the slip plane, and a unit vector $\mathbf{m}^\alpha$ denoting the slip direction. The slip systems $(\mathbf{m}^\alpha, \mathbf{n}^\alpha)$ are assumed to be known. (*iv*) The slip system deformation resistance $s^\alpha > 0$, with dimensions of stress. The quantities s^α represent averaged slip system resistances to crystallographic glide offered by the underlying strengthening mechanisms such as intrinsic lattice resistance, solid solution strengthening, forest dislocation densities, subgrains, etc.

We assume that the velocity gradient $\mathbf{L}$ is specified, and the constitutive model that we shall consider consists of a coupled set of evolution equations for the state variables $\{\mathbf{T}, (\mathbf{m}^\alpha, \mathbf{n}^\alpha), s^\alpha\}$.

The incremental deformation of a crystal is taken as the sum of contributions from two independent atomic mechanisms: (*i*) an overall "elastic" distortion of the lattice, and (*ii*) "plastic" simple shears that do not disturb the lattice geometry. Accordingly, the macroscopic velocity gradient $\mathbf{L}$ is taken to be additively decomposable into an elastic and

a plastic part:

$$\mathbf{L} = \mathbf{L}^e + \mathbf{L}^p, \tag{2.1}$$

and that $\mathbf{L}^p$ is given as the sum of the shearing rates on all the slip systems

$$\mathbf{L}^p = \sum_\alpha \dot{\gamma}^\alpha \operatorname{sign}(\tau^\alpha)\, \mathbf{S}^\alpha, \quad \text{with} \quad \dot{\gamma}^\alpha \geq 0, \tag{2.2}$$

where

$$\mathbf{S}^\alpha = \mathbf{m}^\alpha \otimes \mathbf{n}^\alpha \tag{2.3}$$

is the Schmid tensor, and

$$\tau^\alpha = \mathbf{m}^\alpha \cdot \mathbf{T}\mathbf{n}^\alpha = \mathbf{T} \cdot \mathbf{S}^\alpha \tag{2.4}$$

denotes the resolved shear stress, or the Schmid stress on the slip system α. With this, the elastic and plastic stretching and spin tensors are denoted by

$$\mathbf{D}^e = \operatorname{sym}\mathbf{L}^e, \tag{2.5}$$

$$\mathbf{W}^e = \operatorname{skw}\mathbf{L}^e, \tag{2.6}$$

$$\mathbf{D}^p = \sum_\alpha \dot{\gamma}^\alpha \operatorname{sign}(\tau^\alpha)\, \mathbf{P}^\alpha, \quad \text{with} \quad \mathbf{P}^\alpha = \operatorname{sym}\mathbf{S}^\alpha, \tag{2.7}$$

$$\mathbf{W}^p = \sum_\alpha \dot{\gamma}^\alpha \operatorname{sign}(\tau^\alpha)\, \mathbf{Q}^\alpha, \quad \text{with} \quad \mathbf{Q}^\alpha = \operatorname{skw}\mathbf{S}^\alpha, \tag{2.8}$$

respectively.

The lattice corotational rate of the Cauchy stress is denoted by

$$\mathbf{T}^{\nabla e} = \dot{\mathbf{T}} - \mathbf{W}^e\mathbf{T} + \mathbf{T}\mathbf{W}^e, \tag{2.9}$$

and assuming that the *elastic stretches are small*, the evolution equation for $\mathbf{T}$ is taken as

$$\mathbf{T}^{\nabla e} = \boldsymbol{\mathcal{C}}[\mathbf{D}^e] = \boldsymbol{\mathcal{C}}[\mathbf{D}] - \sum_\alpha \dot{\gamma}^\alpha \operatorname{sign}(\tau^\alpha)\, \boldsymbol{\mathcal{C}}[\mathbf{P}^\alpha], \quad \text{with} \quad \dot{\gamma}^\alpha \geq 0, \tag{2.10}$$

where $\boldsymbol{\mathcal{C}}$ is a fourth order elasticity tensor. The conditions under which a slip system is inactive, $\dot{\gamma}^\alpha = 0$, or active, $\dot{\gamma}^\alpha > 0$, are based on the following yield and unloading/loading criteria. The actual magnitudes of $\dot{\gamma}^\alpha$ for the active systems are determined by the consistency condition to be considered shortly.

The yield conditions of the rate-independent crystal plasticity problem are $|\tau^\alpha| \leq s^\alpha$. The planes $|\tau^\alpha| = s^\alpha$ denote the facets of the current pyramidal yield surface in stress space, and $\{\text{sign}(\tau^\alpha)\mathbf{P}^\alpha\}$ denotes the outward unit normal to each facet. If $|\tau^\alpha| < s^\alpha$, or if $|\tau^\alpha| = s^\alpha$ and a *trial stress rate* $\boldsymbol{\mathcal{C}}[\mathbf{D}]$ points to the interior side of the yield facet, that is, if $\{\text{sign}(\tau^\alpha)\mathbf{P}^\alpha\} \cdot \boldsymbol{\mathcal{C}}[\mathbf{D}] \leq 0$, then the slip system is *inactive* and $\dot{\gamma}^\alpha = 0$. A slip system is *potentially active*, that is $\dot{\gamma}^\alpha \geq 0$, if $|\tau^\alpha| = s^\alpha$ and $\{\text{sign}(\tau^\alpha)\mathbf{P}^\alpha\} \cdot \boldsymbol{\mathcal{C}}[\mathbf{D}] > 0$. To summarize,

$$\dot{\gamma}^\alpha = \left\{ \begin{array}{ll} 0 & \text{if } |\tau^\alpha| < s^\alpha, \text{ or if } |\tau^\alpha| = s^\alpha \text{ and } \{\text{sign}(\tau^\alpha)\mathbf{P}^\alpha\} \cdot \boldsymbol{\mathcal{C}}[\mathbf{D}] \leq 0\ , \\ \geq 0 & \text{if } |\tau^\alpha| = s^\alpha \text{ and } \{\text{sign}(\tau^\alpha)\mathbf{P}^\alpha\} \cdot \boldsymbol{\mathcal{C}}[\mathbf{D}] > 0\ . \end{array} \right\} \tag{2.11}$$

We denote by

$$\mathcal{PA} = \{\alpha \,|\alpha = 1, \cdots, n\}$$

the n *potentially active* slip systems. Of the n potentially active systems the $m \leq n$ systems for which the shear rates are actually non-zero are the *active* systems, and we donote the set of active systems by

$$\mathcal{A} = \{\alpha \,|\alpha = 1, \cdots, m \leq n\}\,.$$

The orientation of the slip systems is taken to evolve as

$$\dot{\mathbf{m}}^\alpha = \mathbf{W}^e\,\mathbf{m}^\alpha, \quad \text{and} \quad \dot{\mathbf{n}}^\alpha = \mathbf{W}^e\,\mathbf{n}^\alpha, \tag{2.12}$$

and the evolution equations for the slip resistances are taken as

$$\dot{s}^\alpha = \sum_\beta h^{\alpha\beta}\,\dot{\gamma}^\beta, \tag{2.13}$$

where $h^{\alpha\beta}$ are the hardening moduli which describe the rate of increase of the deformation resistance on slip system α due to shearing on slip system β. The matrix $\left[h^{\alpha\beta}\right]$ describes both self hardening and latent hardening of the slip systems.

Finally, during plastic flow the active systems must satisfy the consistency condition

$$\dot{\overline{|\tau^\alpha|}} = \dot{s}^\alpha, \tag{2.14}$$

and for inactive systems the condition

$$\dot{\overline{|\tau^\alpha|}} < \dot{s}^\alpha \tag{2.15}$$

must hold. Using equations (2.4), (2.9), and (2.12) we obtain

$$\dot{\overline{|\tau^\alpha|}} = \dot{\overline{|\mathbf{m}^\alpha \cdot \mathbf{T}\mathbf{n}^\alpha|}} = \{\text{sign}(\tau^\alpha)\mathbf{P}^\alpha\} \cdot \mathbf{T}^{\nabla e}. \tag{2.16}$$

Substituting (2.16) and the evolution equations for the stress (2.10) and the slip resistances (2.13) in the consistency condition (2.14), gives the following set of equations for the evolution equations for the state variables $\{\mathbf{T}, (\mathbf{m}^\alpha, \mathbf{n}^\alpha), s^\alpha\}$ to be "consistent":

$$\sum_{\beta \in \mathcal{A}} A^{\alpha\beta}\, x^\beta = b^\alpha, \qquad \alpha \in \mathcal{A}, \tag{2.17}$$

with

$$A^{\alpha\beta} = h^{\alpha\beta} + \text{sign}(\tau^\alpha)\,\text{sign}(\tau^\beta)\,\mathbf{P}^\alpha \cdot \boldsymbol{\mathcal{C}}\left[\mathbf{P}^\beta\right], \tag{2.18}$$

$$b^\alpha = \{\text{sign}(\tau^\alpha)\mathbf{P}^\alpha\} \cdot \boldsymbol{\mathcal{C}}[\mathbf{D}] > 0, \tag{2.19}$$

$$x^\beta \equiv \dot{\gamma}^\beta > 0. \tag{2.20}$$

Equation (2.17) is a system of linear equations for $x^\beta \equiv \dot{\gamma}^\beta > 0$. However, we do not know the elements of the set $\mathcal{A}$. These are determined in the following iterative fashion. Since we do know the potentially active systems, we assume that all the potentially active systems are active, extend the equations in (2.17) to

$$\sum_{\beta \in \mathcal{PA}} A^{\alpha\beta}\, x^\beta = b^\alpha, \qquad \alpha \in \mathcal{PA}, \tag{2.21}$$

and solve this linear system of equations $Ax = b$, with A an $n \times n$ matrix, for the vector of shear rates x, looking for elements

$$x^\beta = \dot{\gamma}^\beta > 0.$$

If for any system the solution

$$x^\beta = \dot{\gamma}^\beta \leq 0,$$

then this system is inactive, we remove it from our list of active systems, redefine our reduced system $Ax = b$, and solve the linear system of equations until all

$$x^\beta = \dot{\gamma}^\beta > 0.$$

This iterative solution procedure determines the active slip systems and the corresponding slip increments.

At each stage of our iterative procedure the linear equations $Ax = b$ are solved as follows. Recall that the *range*, *null space*, and *rank* of a matrix $A \in \mathcal{R}^{n\times n}$ are respectively defined by:

Range of A: $R(A) = \{y \in \mathcal{R}^n \mid y = Ax \text{ for some } x \in \mathcal{R}^n\}$,

Null Space of A: $N(A) = \{x \in \mathcal{R}^n \mid Ax = 0\}$,

Rank of A: $r = \text{rank}(A) = \dim[R(A)]$.

If A has rank $r = n$, then it is non-singular. If A has rank $r < n$, then it is singular, and in this case $N(A) \neq \{0\}$, and $\dim[N(A)] = n - r$.

The problem concerning us is how to find $x \in \mathcal{R}^n$ such that $Ax = b$, where $A \in \mathcal{R}^{n\times n}$ and $b \in \mathcal{R}^n$ are given. As is well known (e.g., Golub and Van Loan, 1989), this problem has a solution if and only if $b \in R(A)$, and it is unique if and only if $N(A) = \{0\}$.

For the rate-independent crystal plasticity problem formulated above, we assume that $b \in R(A)$, that is a solution exists. However, because of the typical multiplicity of slip systems in ductile crystals we expect that for certain crystal orientations and loading conditions the matrix A may be singular, that is $N(A) \neq \{0\}$. In this case the singular set of equations $Ax = b$ does have a solution x, but it is non-unique. To obtain uniqueness we pick the vector x with the *smallest length* $||x|| = \left(x^T x\right)^{1/2}$. Such a solution is obtained by the use of the powerful singular value decomposition — the SVD — of the matrix A .

A *singular value decomposition* (SVD) of an $n \times n$ real matrix A is a factorization of the form (e.g. Golub and Van Loan, 1989; Press *et al.*, 1989; Strang, 1989):

$$A = Q_1 \, \Sigma \, Q_2^T, \tag{2.22}$$

where

$$Q_1^T Q_1 = Q_2^T Q_2 = I_n, \quad \text{and} \quad \Sigma = \text{diag}\,(\sigma_1, \cdots, \sigma_n) \quad \text{with} \quad \sigma_1 \geq \sigma_2 \geq \cdots \geq \sigma_n \geq 0. \tag{2.23}$$

The columns of Q_1 are orthonormalized eigenvectors of AA^T, and the columns of Q_2 are orthonormalized eigenvectors of A^TA. The diagonal elements of Σ are the non-negative square roots of the eigenvalues of both AA^T and A^TA, and are called the *singular values* of A.

The decomposition (2.22) is "almost" unique. That is, it is unique up to (i) making the same permutation of the columns of Q_1, elements of Σ, and columns of Q_2 (or rows of Q_2^T), or (ii) forming linear combinations of any columns of Q_1 and Q_2 whose corresponding elements of Σ happen to be exactly equal. By forcing the ordering of the singular values shown in (2.23), the first of these possibilities leading to a lack of uniqueness is mitigated.

In terms of the singular value decomposition, the rank r of a matrix A is the number of nonzero singular values. Thus if $\text{rank}(A) = r$, then $\sigma_{r+1} = \sigma_{r+2} = \cdots = \sigma_n = 0$.

Let $A = Q_1 \Sigma Q_2^T$ be the singular value decomposition of A, then the *pseudoinverse* of A is defined by

$$A^+ \equiv Q_2 \Sigma^+ Q_1^T, \quad \text{with} \quad \Sigma^+ = \text{diag}\left(\sigma_i^+\right), \tag{2.24}$$

where

$$\sigma_i^+ = \left\{ \begin{array}{lll} 1/\sigma_i & \text{for} & \sigma_i > 0, \\ 0 & \text{for} & \sigma_i = 0. \end{array} \right\} \tag{2.25}$$

If A is square and nonsingular, then all its singular values are nonzero. In this case A is invertible with inverse $A^{-1} = A^+$, and $Ax = b$ has one and only one solution $x = A^+b = A^{-1}b$. That is, the pseudoinverse is the same as the inverse when A is invertible.

Let $b \in R(A)$ be a given vector, and suppose we wish to determine a vector x such that $Ax = b$ when A is singular. In this case there is no unique solution. Then, we seek a solution x^+ amongst all x which satisfy $Ax = b$ such that

$$||x^+|| = \min.$$

Such a solution is given by :

$$x^+ = A^+b, \tag{2.26}$$

and it is *unique*[1] (e.g. Golub and Van Loan, 1989; Press et al., 1989; Strang, 1989). All other solutions x have some component from the null space $N(A)$. The length squared

[1]Well "almost" unique, since as discussed earlier, the SVD decomposition of A is "almost" unique.

of any such x will be equal to the length squared of x^+ added to length squared of the nullspace component — which can only increase length over that of x^+.

We adopt x^+ as our solution to the the linear problem (2.21) at each stage of our iterative procedure to determine the active slip systems and the corresponding slip increments.

REMARK 1: Hill and Rice (1972) have shown that if the matrix A with elements

$$A^{\alpha\beta} = h^{\alpha\beta} + \text{sign}(\tau^\alpha)\,\text{sign}(\tau^\beta)\,\mathbf{P}^\alpha \cdot \boldsymbol{\mathcal{C}}\left[\mathbf{P}^\beta\right] \tag{2.27}$$

defined over the active systems is positive definite, then one always obtains a unique set of slip rates. There have been numerous attempts at formulating equations for the hardening moduli $h^{\alpha\beta}$ to ensure that A is positive definite to guarantee a unique set of slip rates (e.g., Bassani and Wu, 1991; Havner, 1992; Bassani, 1994). However, since the slip system hardening moduli $h^{\alpha\beta}$ are typically three orders of magnitude smaller than the incremental elastic moduli $\boldsymbol{\mathcal{C}}$, the second term in (2.27) dominates, and the uniqueness (or lack thereof) of the $\dot{\gamma}^\alpha$, is dominated by the multiplicity of the slip systems and the corresponding interdependence of the tensors $\mathbf{P}^\alpha$ and $\mathbf{P}^\beta$. Any robust solution scheme for rate-independent crystal plasticity should not depend heavily on a precise knowledge of the hardening moduli $h^{\alpha\beta}$ which, as mentioned previously, are the least well characterized part of the constitutive model. We shall show that our computational scheme for calculating the shear rates $\dot{\gamma}^\alpha$ works for essentially arbitrary, $h^{\alpha\beta}$, including the technically important non-hardening case $h^{\alpha\beta} = 0$.

REMARK 2: The smallest length solution x^+ is reminiscent of Taylor's early but incomplete method of determining the amount of slip rates $\dot{\gamma}^\alpha$ on the active slip systems. In the rigid-plastic, non-hardening theory, Taylor made the assumption that each crystal will slip on that combination of systems which makes the incremental work the least. Then from his additional assumption of equal positive slip resistances for every slip system he deduced his *principle of minimum incremental shears*. His most concise statement of this for f.c.c. crystals is in Taylor (1938b, p.229):

> " Of all the possible combinations of the 12 shears which could produce an assigned strain, only that combination is operative for which the sum of the absolute values of the shears is the least."

Now, the $p-norms$ of any vector $x \in \mathcal{R}^n$ are defined by (e.g. Golub and Van Loan,

1989)

$$||x||_p = (|x_1|^p + \cdots + |x_n|^p)^{1/p}, \qquad p \geq 1,$$

of which

$$||x||_1 = (|x_1| + \cdots + |x_n|),$$

and

$$||x||_2 = \left(|x_1|^2 + \cdots + |x_n|^2\right)^{1/2} = (x^T x)^{1/2}$$

are two important special cases. Also, these two norms satisfy the inequality

$$||x||_2 \leq ||x||_1 .$$

Thus the $||x||_2 = (x^T x)^{1/2}$ norm of our solution x^+ is also smaller than or equal to the $||x||_1 = (|x_1| + \cdots + |x_n|)$ norm of Taylor's[2].

---

[2]In Taylor's original formulation it was not clear that the yield criterion was satisfied on all active slip systems, and not violated on the inactive systems. Later, Chin and Mammel (1969) rephrased Taylor's method for determining the active slip systems and the amount of shear rates $\dot{\gamma}^\alpha > 0$ on these systems in terms of an optimization problem of linear programming. In particular, with $s^\alpha > 0$ denoting the deformation resistance of a slip system, and $\dot{\gamma}^\alpha \geq 0$ the corresponding shearing rate, they showed that Taylor's method of determining the active slip systems consists of minimizing the "internal rate of work"

$$W(\dot{\gamma}) = \sum_\alpha s^\alpha \dot{\gamma}^\alpha$$

subject to the constraints

$$\mathbf{C}(\dot{\gamma}) = \mathbf{D} - \sum_\alpha \dot{\gamma}^\alpha \text{sign}\,(\tau^\alpha)\,\mathbf{P}^\alpha = \mathbf{0},$$

where $\mathbf{D}$ is the imposed stretching tensor. The minimum rate of work is obtained as the saddle value of the Lagrangian function

$$F(\dot{\gamma}, \Lambda) = W(\dot{\gamma}) + \Lambda \cdot \mathbf{C}(\dot{\gamma}),$$

where Λ is a Lagrange multiplier. To obtain the saddle point one finds $(\dot{\gamma}_0, \Lambda_0)$ such that

$$\frac{\partial}{\partial \Lambda} F\Big|_0 = \mathbf{D} - \sum_\alpha \dot{\gamma}_0^\alpha \,\text{sign}(\tau^\alpha)\,\mathbf{P}^\alpha = \mathbf{0} \tag{2.28}$$

$$\frac{\partial}{\partial \dot{\gamma}^\alpha} F\Big|_0 = s^\alpha - \text{sign}(\tau^\alpha)\,\Lambda_0 \cdot \mathbf{P}^\alpha = \left\{ \begin{array}{ll} \geq 0 & \text{always} \\ = 0 & \text{if } \dot{\gamma}_0^\alpha > 0 \end{array} \right\}. \tag{2.29}$$

The inequalities (2.29) are equivalent to

$$s^\alpha - |\tau_0^\alpha| = \left\{ \begin{array}{ll} \geq 0 & \text{always} \\ = 0 & \text{if } \dot{\gamma}_0^\alpha > 0 \end{array} \right\}, \tag{2.30}$$

with the Lagrange multiplier Λ_0 identified as the stress $\mathbf{T}_0$. Hence in order to obtain a set of shear rates $\dot{\gamma}^\alpha$ that minimizes the internal rate of work $W(\dot{\gamma})$, there exists a stress $\mathbf{T}$ which obeys the yield conditions, and which attains the critical value s^α on the systems where slip occurs ($\dot{\gamma}_0^\alpha > 0$), and does not exceed it on the inactive systems ($\dot{\gamma}_0^\alpha = 0$). Although it was unrecognized by Taylor, this restriction is part of the minimum rate of work analysis.

Note that such a solution is still non-unique, whereas the minimum length solution x^+ obtained by using the SVD method to solve our previously formulated linear system $Ax = b$ is unique.

Chapter 3

An Incremental Formulation Of The Constitutive Model

Here, we present an *incremental* version of the rate-independent constitutive model for crystal elasto-plasticity. The major differences between the model considered here and that presented in the previous section are that (*i*) instead of the additive decomposition of the velocity gradient into an elastic and plastic part, $\mathbf{L} = \mathbf{L}^e + \mathbf{L}^p$, we use a multiplicative decomposition of the deformation gradient into an elastic and plastic part, $\mathbf{F} = \mathbf{F}^e\,\mathbf{F}^p$, and (*ii*) instead of the rate constitutive equation $\mathbf{T}^{\nabla e} = \boldsymbol{\mathcal{C}}\,[\mathbf{D}^e]$ for the stress, we shall use a total, hyperelastic constitutive equation for the stress. For infinitesimal elastic stretches, the two formulations may be shown to be equivalent. However, the incremental formulation developed here is suitable for direct numerical implementation in displacement based finite element programs, and it has the additional advantage that one does not have to develop an "incrementally objective time integration procedure" for it (c.f., e.g., Weber *et al.*, 1990), the time integration scheme arising naturally from the incremental model automatically satisfies this important requirement.

The governing variables of the model are: (*i*) The Cauchy stress, $\mathbf{T}$. (*ii*) The deformation gradient, $\mathbf{F}$. (*iii*) Crystal slips systems, labeled by integers α. Each slip system is specified by a unit normal $\mathbf{n}_o^\alpha$ to the slip plane, and a unit vector $\mathbf{m}_o^\alpha$ denoting the slip direction. The slip systems $(\mathbf{m}_o^\alpha, \mathbf{n}_o^\alpha)$ are assumed to be known in the reference configuration. (*iv*) The plastic deformation gradient, $\mathbf{F}^p$, with $\det\mathbf{F}^p = 1$. The local configuration defined by $\mathbf{F}^p$ is relaxed, that is $\mathbf{T} = \mathbf{0}$, and is chosen such that the crystal lattice in this configuration

has the same orientation with respect to a fixed orthonormal basis in space as it had in the reference configuration. Following Mandel (1974), such a local configuration is called an *isoclinic relaxed configuration.* (v) The slip system deformation resistance $s^\alpha > 0$, with units of stress.

In terms of $\mathbf{F}$ and $\mathbf{F}^p$ the quantity

$$\mathbf{F}^e \equiv \mathbf{F}\,\mathbf{F}^{p-1} \tag{3.1}$$

defines an elastic deformation gradient.

Let t denote the current time, Δt an infinitesimal time increment, and $\tau = t + \Delta t$. We take as given $(\mathbf{F}(t), \mathbf{F}(\tau))$, and $(\mathbf{m}_o^\alpha, \mathbf{n}_o^\alpha)$, $\{\mathbf{T}(t), \mathbf{F}^p(t), s^\alpha(t)\}$. Then the incremental problem is to calculate $\{\mathbf{T}(\tau), \mathbf{F}^p(\tau), s^\alpha(\tau)\}$, and the orientation of the slip systems in the deformed configuration at time τ from

$$\begin{aligned} \mathbf{m}_\tau^\alpha &= \mathbf{F}^e(\tau)\mathbf{m}_o^\alpha, \\ \mathbf{n}_\tau^\alpha &= \mathbf{F}^e(\tau)^{-T}\mathbf{n}_o^\alpha, \end{aligned}$$

and march forward in time.

For metallic materials the elastic stretch is usually infinitesimal, and accordingly the constitutive equation for stress may be taken as a linear relation

$$\mathbf{T}^*(\tau) = \boldsymbol{\mathcal{C}}\,[\mathbf{E}^e(\tau)]\,, \tag{3.2}$$

where $\boldsymbol{\mathcal{C}}$ is a fourth order elasticity tensor. With

$$\mathbf{C}^e(\tau) = (\mathbf{F}^e(\tau))^T\mathbf{F}^e(\tau), \tag{3.3}$$

defining an elastic right Cauchy-Green tensor,

$$\mathbf{E}^e(\tau) = (1/2)\,\{\mathbf{C}^e(\tau) - 1\} \tag{3.4}$$

is an elastic strain measure, and

$$\mathbf{T}^*(\tau) = \mathbf{F}^e(\tau)^{-1}\,\{(\det\mathbf{F}^e(\tau))\;\mathbf{T}(\tau)\}\;\mathbf{F}^e(\tau)^{-T} \tag{3.5}$$

is a stress measure elastic power conjugate to the strain measure (3.4).

The tensor product

$$\mathbf{S}_0^\alpha = \mathbf{m}_o^\alpha \otimes \mathbf{n}_o^\alpha \tag{3.6}$$

is called the Schmid tensor for the slip system α, and the scalar

$$\tau^\alpha(\tau) = \{\mathbf{C}^e(\tau)\,\mathbf{T}^*(\tau)\} \cdot \mathbf{S}_0^\alpha \tag{3.7}$$

is the resolved shear stress, or the Schmid stress, on the slip system α at time τ. For infinitesimal elastic stretches the resolved shear stress $\tau^\alpha(\tau)$ may be approximated by

$$\tau^\alpha(\tau) \doteq \mathbf{T}^*(\tau) \cdot \mathbf{S}_o^\alpha \tag{3.8}$$

Next, we define a *trial* elastic strain and stress at time τ as follows. We fix the value of $\mathbf{F}^p$ at time t, and define a trial elastic deformation gradient by

$$\mathbf{F}^e(\tau)^{\mathrm{tr}} = \mathbf{F}(\tau)\,\mathbf{F}^p(t)^{-1}, \tag{3.9}$$

in terms of which we define a trial elastic right Cauchy-Green tensor by

$$\mathbf{C}^e(\tau)^{\mathrm{tr}} = (\mathbf{F}^e(\tau)^{\mathrm{tr}})^T \mathbf{F}^e(\tau)^{\mathrm{tr}}, \tag{3.10}$$

a trail elastic strain by

$$\mathbf{E}^e(\tau)^{\mathrm{tr}} = (1/2)\left\{\mathbf{C}^e(\tau)^{\mathrm{tr}} - \mathbf{1}\right\}, \tag{3.11}$$

a trial stress by

$$\mathbf{T}^*(\tau)^{\mathrm{tr}} = \mathcal{C}\left[\mathbf{E}^e(\tau)^{\mathrm{tr}}\right], \tag{3.12}$$

and a trial resolved shear stress by

$$\tau^\alpha(\tau)^{\mathrm{tr}} = \mathbf{T}^*(\tau)^{\mathrm{tr}} \cdot \mathbf{S}_0^\alpha. \tag{3.13}$$

We make the important physical assumption that

$$\mathrm{sign}\,(\tau^\alpha(\tau)) = \mathrm{sign}\left(\tau^\alpha(\tau)^{\mathrm{tr}}\right). \tag{3.14}$$

With these definitions, the incremental flow rule is taken as

$$\mathbf{F}^p(\tau) = \left\{ 1 + \sum_\alpha \Delta\gamma^\alpha \operatorname{sign}\left(\tau^\alpha(\tau)^{\mathrm{tr}}\right) \mathbf{S}_0^\alpha \right\} \mathbf{F}^p(t), \tag{3.15}$$

with

$$\Delta\gamma^\alpha = \left\{ \begin{array}{ll} 0 & \text{if} \quad \left|\tau^\alpha(\tau)^{\mathrm{tr}}\right| \leq s^\alpha(t), \\ \\ \geq 0 & \text{if} \quad \left|\tau^\alpha(\tau)^{\mathrm{tr}}\right| > s^\alpha(t). \end{array} \right\} \tag{3.16}$$

Systems for which

$$\left|\tau^\alpha(\tau)^{\mathrm{tr}}\right| \leq s^\alpha(t),$$

are *inactive*, and those for which

$$\left|\tau^\alpha(\tau)^{\mathrm{tr}}\right| > s^\alpha(t),$$

are *potentially active*. As before, we denote by

$$\mathcal{PA} = \{\alpha \,|\alpha = 1, \cdots, n\}$$

the *n potentially active* slip systems. Of the n potentially active systems, the $m \leq n$ systems for which the shear increments are actually non-zero are the *active* systems, and we donote the set of active systems by

$$\mathcal{A} = \{\alpha \,|\alpha = 1, \cdots, m \leq n\}.$$

Next, the evolution equation for the slip resistances are taken as

$$s^\alpha(\tau) = s^\alpha(t) + \sum_{\beta \in \mathcal{A}} h^{\alpha\beta}(t)\, \Delta\gamma^\beta, \quad \alpha = 1, \cdots, N, \tag{3.17}$$

where $h^{\alpha\beta}$ are the hardening moduli, and N is the total number of slip systems.

Finally, during plastic flow the active systems must satisfy the consistency condition

$$|\tau^\alpha(\tau)| = s^\alpha(\tau), \tag{3.18}$$

and for inactive systems the condition

$$|\tau^\alpha(\tau)| < s^\alpha(\tau), \tag{3.19}$$

must hold.

Retaining terms of first order in $\Delta\gamma^\beta$, it is straightforward to show that

$$\begin{aligned} |\tau^\alpha(\tau)| &= \left|\tau^\alpha(\tau)^{\mathrm{tr}}\right| - \\ &\quad \sum_{\beta\in\mathcal{A}} \left\{\mathrm{sign}\left(\tau^\alpha(\tau)^{\mathrm{tr}}\right)\mathrm{sign}\left(\tau^\beta(\tau)^{\mathrm{tr}}\right)\right. \\ &\quad\quad \left.\mathbf{S}_0^\alpha \cdot \boldsymbol{\mathcal{C}}\left[\mathrm{sym}\left(\mathbf{C}^e(\tau)^{\mathrm{tr}}\mathbf{S}_0^\beta\right)\right]\right\}\Delta\gamma^\beta, \end{aligned} \tag{3.20}$$

use of which in the consistency condition (3.18) gives

$$\sum_{\beta\in\mathcal{A}} A^{\alpha\beta}\, x^\beta = b^\alpha, \qquad \alpha \in \mathcal{A}, \tag{3.21}$$

with

$$\begin{aligned} A^{\alpha\beta} &= h^{\alpha\beta}(t) + \\ &\quad \mathrm{sign}\left(\tau^\alpha(\tau)^{\mathrm{tr}}\right)\mathrm{sign}\left(\tau^\beta(\tau)^{\mathrm{tr}}\right)\mathbf{S}_0^\alpha \cdot \boldsymbol{\mathcal{C}}\left[\mathrm{sym}\left(\mathbf{C}^e(\tau)^{\mathrm{tr}}\mathbf{S}_0^\beta\right)\right], && (3.22) \\ b^\alpha &= \left|\tau^\alpha(\tau)^{\mathrm{tr}}\right| - s^\alpha(t) > 0, && (3.23) \\ x^\beta &\equiv \Delta\gamma^\beta > 0. && (3.24) \end{aligned}$$

Equation (3.21) is a system of linear equations for $x^\beta \equiv \Delta\gamma^\beta > 0$.

Apart from the presence of a small elastic stretch related term $\mathbf{C}^e(\tau)^{\mathrm{tr}}$, this system of linear equations (3.21) is similar to the system (2.17), and the iterative solution procedure to determine the active slip systems and the corresponding slip increments developed in the previous section applies here as well. The procedure is summarized below.

Let t denote the current time, Δt an infinitesimal time increment, and $\tau = t + \Delta t$. Then, Given : (1) $\mathbf{F}(t), \mathbf{F}(\tau)$; (2) $(\mathbf{m}_0^\alpha, \mathbf{n}_0^\alpha)$ — time independent quantities; and (3) $\{\mathbf{F}^p(t), s^\alpha(t), \mathbf{T}(t)\}$.

Calculate : (a) $\{\mathbf{F}^p(\tau), s^\alpha(\tau), \mathbf{T}(\tau)\}$; and (b) the orientation of the slip system in the

deformed configuration at at time τ from

$$\begin{aligned} \mathbf{m}_\tau^\alpha &= \mathbf{F}^e(\tau)\mathbf{m}_0^\alpha, \\ \mathbf{n}_\tau^\alpha &= \mathbf{F}^{e^{-T}}(\tau)\mathbf{n}_0^\alpha, \end{aligned}$$

and march forward in time. The steps used in the calculation procedure are:

Step 1. Calculate the trial elastic strain $\mathbf{E}^e(\tau)^{tr}$:

$$\begin{aligned} \mathbf{F}^e(\tau)^{\mathrm{tr}} &= \mathbf{F}(\tau)\,\mathbf{F}^p(t), \\ \mathbf{C}^e(\tau)^{\mathrm{tr}} &= (\mathbf{F}^e(\tau)^{\mathrm{tr}})^T\mathbf{F}^e(\tau)^{\mathrm{tr}}, \\ \mathbf{E}^e(\tau)^{\mathrm{tr}} &= (1/2)\{\mathbf{C}^e(\tau)^{\mathrm{tr}} - \mathbf{1}\}. \end{aligned} \tag{3.25}$$

Step 2. Calculate the trial stress $\mathbf{T}^*(\tau)^{\mathrm{tr}}$:

$$\mathbf{T}^*(\tau)^{\mathrm{tr}} = \mathcal{C}[\mathbf{E}^e(\tau)^{\mathrm{tr}}].$$

Step 3. Calculate the trial resolved shear stress $\tau^\alpha(\tau)^{\mathrm{tr}}$ on each slip system :

$$\begin{aligned} \mathbf{S}_o^\alpha &= \mathbf{m}_0^\alpha \otimes \mathbf{n}_0^\alpha, \\ \tau^\alpha(\tau)^{\mathrm{tr}} &= \mathbf{T}^*(\tau)^{\mathrm{tr}} \cdot \mathbf{S}_o^\alpha. \end{aligned}$$

Step 4. Determine the set $\mathcal{PA}$ of the n potentially active slip systems which satisfy

$$|\tau^\alpha(\tau)^{\mathrm{tr}}| - s^\alpha(t) > 0.$$

Step 5. Calculate the shear increments from the consistency condition using the SVD method as :

$$x^+ = A^+ b,$$

where A^+ is the pseudoinverse of the matrix of the $n \times n$ matrix A, defined over all

the potentially active slip systems, with elements with

$$\begin{aligned} A^{\alpha\beta} &= h^{\alpha\beta}(t) + \text{sign}\,(\tau^{\alpha}(\tau)^{\text{tr}})\ \text{sign}\,(\tau^{\beta}(\tau)^{\text{tr}})\,\mathbf{S}_o^{\alpha}\cdot\mathcal{C}[\text{sym}\,(\mathbf{C}^e(\tau)^{\text{tr}}\mathbf{S}_o^{\beta})], \\ b^{\alpha} &= |\tau^{\alpha}(\tau)^{\text{tr}}| - s^{\alpha}(t), \\ x^{\beta} &\equiv \Delta\gamma^{\beta} > 0. \end{aligned}$$

If for any system the solution $x^{\beta} = \Delta\gamma^{\beta} \leq 0$, then this system is inactive; remove it from the set of potentially active slip systems by removing the βth row and column of A and the βth row of b, redefine the reduced system $Ax = b$, and solve the linear system of equations until all $x^{\beta} = \Delta\gamma^{\beta} > 0$. The size of A at the end of this step is $m \times m$, where m is the number of active slip systems.

Step 6. Update the plastic deformation gradient $\mathbf{F}^p(\tau)$:

$$\mathbf{F}^p(\tau) = \{\mathbf{1} + \sum_{\alpha=1}^{m} \text{sign}\,(\tau^{\alpha}(\tau)^{\text{tr}})\Delta\gamma^{\alpha}\mathbf{S}_o^{\alpha}\}\mathbf{F}^p(t).$$

Step 7. Check if $\det \mathbf{F}^p(\tau) = 1$. If not, normalize $\mathbf{F}^p(\tau)$ as :

$$\mathbf{F}^p(\tau) = [\det\mathbf{F}^p(\tau)]^{-1/3}\,\mathbf{F}^p(\tau).$$

Step 8. Compute the elastic deformation gradient $\mathbf{F}^e(\tau)$ and the stress $\mathbf{T}^*(\tau)$:

$$\begin{aligned} \mathbf{F}^e(\tau) &= \mathbf{F}(\tau)\mathbf{F}^{p^{-1}}(\tau) \\ \mathbf{T}^*(\tau) &= \mathbf{T}^e(\tau)^{\text{tr}} - \sum_{\alpha=1}^{m} \{\,\Delta\gamma^{\alpha}\,\text{sign}\,(\tau^{\alpha}(\tau)^{\text{tr}})\,\}\,\mathcal{C}[\text{sym}\,(\mathbf{C}^e(\tau)^{\text{tr}}\mathbf{S}_o^{\alpha})]. \end{aligned}$$

Step 9. Update the variables $\{\mathbf{T}(\tau), s^{\alpha}(\tau)\}$:

$$\begin{aligned} \mathbf{T}(\tau) &= \mathbf{F}^e(\tau)\,\{[\det\mathbf{F}^e(\tau)]^{-1}\,\mathbf{T}^*(\tau)\}\,\mathbf{F}^{e^T}(\tau) \\ s^{\alpha}(\tau) &= s^{\alpha}(t) + \sum_{\beta=1}^{m} h^{\alpha\beta}\,\Delta\gamma^{\beta}, \quad \alpha = 1, \cdots, N \end{aligned}$$

Here, N denotes the total number of slip systems. For example, $N = 12$, for an f.c.c. crystal.

Step 10. Check if consistency is satisfied for all the slip systems i.e

$$|\tau^\alpha(\tau)| \;=\; s^\alpha(\tau),$$

if the slip system is active, or

$$|\tau^\alpha(\tau)| \;<\; s^\alpha(\tau) \tag{3.26}$$

if it is inactive. If a particular system, which has previously been deemed to be inactive, does not satisfy this check[1], then include it in the set of potentially active slip systems, go back to step 5 and recompute the shear increments on the active slip systems.

Step 10. Calculate the "texture" $(\mathbf{m}_\tau^\alpha, \mathbf{n}_\tau^\alpha)$:

$$\begin{aligned} \mathbf{m}_\tau^\alpha &= \mathbf{F}^e(\tau)\mathbf{m}_0^\alpha, \\ \mathbf{n}_\tau^\alpha &= \mathbf{F}^{e^{-T}}(\tau)\mathbf{n}_0^\alpha. \end{aligned}$$

The constitutive equations and the time-integration procedures for the rate-independent crystal plasticity model described in this section have been implemented in the commercial finite element program ABAQUS/Standard (1994) by writing a "user material" subroutine UMAT. ABAQUS/Standard requires a "Jacobian Matrix" for the Newton-type iterative method it uses for calculating the equilibriated configuration at the end of a time step. In our implementation we used a quasi-analytical[2] Jacobian (Kalidindi, 1992) employing the rate-dependent constitutive equation (1.1) for the slip increments. The time-integration procedure has also been implemented in ABAQUS/Explicit (1994) by writing a "user material" subroutine VUMAT. Unlike ABAQUS/Standard, the explicit dynamic version ABAQUS/Explicit doesnot require a Jacobian Matrix since no global iterations are involved.

[1] This occasionally occurs at the knee of a load-displacement curve.

[2] Note that an approximate Jacobian has no effect on the accuracy of the solution but only increases the computation time by affecting the rate of convergence of the solution.

Chapter 4

Evaluation of the Rate-Independent Model

In this section, we evaluate the rate-independent model by (a) comparing the predictions of the stress-strain response, the slip system activity and the evolution of the crystal lattice orientation against the predictions of the rate-dependent model of Kalidindi *et al.* (1992) for tension tests on f.c.c. crystals, and (b) comparing the predictions of the stress-strain response and the evolution of the crystallographic texture against the predictions of the rate-dependent Taylor and Finite Element (FEM) model of Kalidindi *et al.* (1992) for a simple compression test on polycrystalline OFHC copper.

For f.c.c. crystals the anisotropic elasticity tensor $\boldsymbol{\mathcal{C}}$ may be specified in terms of three stiffness parameters, C_{11}, C_{12} and C_{44} defined as follows:

$$C_{11} = (\mathbf{e_1}^c \otimes \mathbf{e_1}^c) \cdot \boldsymbol{\mathcal{C}}[\mathbf{e_1}^c \otimes \mathbf{e_1}^c], \tag{4.1}$$

$$C_{12} = (\mathbf{e_1}^c \otimes \mathbf{e_1}^c) \cdot \boldsymbol{\mathcal{C}}[\mathbf{e_2}^c \otimes \mathbf{e_2}^c], \tag{4.2}$$

$$C_{44} = (\mathbf{e_1}^c \otimes \mathbf{e_2}^c) \cdot \boldsymbol{\mathcal{C}}[2 \text{ sym } (\mathbf{e_1}^c \otimes \mathbf{e_2}^c)], \tag{4.3}$$

where $\{\mathbf{e_i}^c | \, i = 1, 2, 3\}$ denotes an orthonormal basis associated with the crystal lattice. In what follows we will consider tension tests on copper single crystals. The values of the elastic parameters for copper are taken as (Simmons and Wang, 1971):

$$C_{11} = 170\,\text{GPa}, \quad C_{12} = 124\,\text{GPa}, \quad C_{44} = 75\,\text{GPa}.$$

For f.c.c. crystals crystallographic slip is assumed to occur on the twelve $\{111\} < 110 >$ slip systems. The components of the slip plane normals and slip directions with respect to an orthonormal basis associated with the crystal lattice, for these slip systems are presented in Table 4.1.

4.1 Tension Test Simulations on f.c.c Single Crystals

We consider two types of crystal hardening behavior:

1. Non-hardening:

$$h^{\alpha\beta} = 0.$$

2. A simple hardening model with moduli:

$$h^{\alpha\beta} = qh^{(\beta)} + \delta_{\alpha\beta}(1-q)h^{(\beta)} \quad \text{(no sum on } \beta\text{)}, \tag{4.4}$$

where $h^{(\beta)}$ is a single slip hardening rate, and q is the latent hardening ratio. The parameter q is taken to be equal to 1.0 for coplanar slip systems, and 1.4 for noncoplanar slip systems (Peirce *et al.*, 1982; Asaro and Needleman, 1985). For the single slip hardening rate, the following specific form is adopted:

$$h^{(\beta)} = h_o\{1 - \frac{s^\beta}{s_s}\}^a, \tag{4.5}$$

where h_o, a and s_s are slip system hardening parameters which are taken to be identical for all slip systems. The values for the slip hardening parameters for single crystal copper are taken as $h_o = 180$ MPa, $s_s = 148$ MPa and $a = 2.25$ for f.c.c. copper single crystals (Kalidindi, 1992).

The initial value of the slip system deformation resistance for both the non-hardening and hardening cases is taken as $s_o = 16$ MPa.

In order to compare the predictions of the rate-independent model against the rate-dependent model, we used the rate-dependent constitutive equation (1.1) for the slip rates, which we repeat below for convinience:

$$\dot{\gamma}^\alpha = \dot{\gamma}_o|\frac{\tau^\alpha}{s^\alpha}|^{1/m}\text{sign}(\tau^\alpha). \tag{4.6}$$

Here $\dot{\gamma}_o$ and m are material parameters, respectively representing a reference shearing rate and the rate sensitivity of slip. The reference shearing rate $\dot{\gamma}_o$ was taken to be equal to $0.001s^{-1}$, and the value of the strain rate sensitivity parameter, m, is set equal to a low value of $m = 0.012$. Recall that the rate independent limit is $m \to 0$.

The single crystal orientations considered are the two corner multi-slip orientations [001] and $[\bar{1}11]$, and a single-slip orientation $[\bar{2}36]$ inside the primary stereographic triangle [001] - [011] - $[\bar{1}11]$ as shown in the Figure 4-1. These initial orientations are specified by three Euler angles $\{\theta, \phi \text{ and } \omega\}$ (Kalidindi, 1992):

Orientation	θ	ϕ	ω
[001]	0.	0.	0.
$[\bar{1}11]$	54.7356	135.0	0.
$[\bar{2}36]$	-31.0	33.7	0.

The simulations on the f.c.c. crystals for the rate independent and the rate dependent models were performed using the FEM package ABAQUS/Implicit. A single eight-noded brick ABAQUS C3D8 element was used to perform the finite element simulations. The simulations were carried out an axial strain rate of $0.001s^{-1}$ to a final true strain of 0.25.

4.1.1 Non-Hardening Case

Figs. 4-2, 4-3 and 4-4 show the stress strain curves, the slip system activities, and the evolution of the crystal orientations obtained from the rate-independent model and the rate-dependent model during tension tests on single crystals with initial orientations [001], $[\bar{1}11]$, and $[\bar{2}36]$, respectively. The results from the rate-independent model are almost indistinguishable from the rate-dependent model.

There are eight slip systems activated in the [001] orientation. The slip activity on all the systems is equal, and the orientation is stable, Fig. 4-2.

There are six slip systems activated in the $[\bar{1}11]$ orientation. The slip activity on all the systems is equal, and the orientation is also stable, Fig. 4-3.

At first there is only slip system $A3 = (111)[\bar{1}01]$ which is activated in the specimen

initially oriented in the $[\bar{2}36]$ direction. During this single slip period the orientation of the tensile axis rotates on a great circle towards the slip direction $[\bar{1}01]$ until it reaches the $[001]-[\bar{1}11]$ boundary of the stereographic triangle around a strain of ~ 0.07, Fig. 4-4c. At this point, the conjugate slip system $B5 = (11\bar{1})[011]$ becomes active[1]. If the crystal were to slip only on the slip system B5, the tensile axis would now rotate towards the conjugate slip direction [011]. However, since there is simultaneous equal slip on the two slip systems A3 and B5, the net result is a slow rotation of the tensile axis along the $[001]-[\bar{1}11]$ boundary of the stereographic triangle towards the limit orientation $[\bar{1}12]$ (which is the vector sum of $[\bar{1}01]$ and [011]), Fig. 4-4c. It is to be noted that for a non-hardening material model the rate-independent and rate-dependent models predict no overshoot of the tensile axis beyond the $[001]-[\bar{1}11]$ boundary. As we shall see in the next section, this is consistent with observations that it is only strong latent hardening that gives rise to overshoot and continued single slip on the original system beyond the $[001]-[\bar{1}11]$ boundary (Havner, 1992).

Note also, that even though the slip systems are non hardening, Fig. 4-4a shows that there is hardening of the macroscopic stress-strain response of the crystal. This hardening is entirely due to the change in the orientation of the crystal.

This analysis shows that the predictions of the rate-independent crystal-plasticity model match those from the rate-dependent model accurately for the orientations inside the primary triangle, as well as the corner multi-slip orientations where the matrix $[A_{\alpha\beta}]$ is singular. In what follows next, the case of a strain-hardening crystal with strong latent hardening is examined.

[1]There is a small difference in the results from the rate-independent and rate-dependent model with regard to the activation of the conjugate slip system B5. In the rate-independent model the activation of the conjugate slip system B5 is abrupt as compared to the smooth activation in the rate-dependent model, Fig. 4-4c. In the rate-dependent model all the slip systems with non-zero resolved shear stress are active. On the other hand, in the rate-independent model a slip system is *potentially active* only if the trial resolved shear stress exceeds the slip deformation resistance on the slip system. This difference in the activation criteria of a slip system is reflected in the lag in the activation of the conjugate slip system B5 in the rate-independent model when compared with the rate-dependent model. The slip system B5 is activated at a strain level of 0.06 in the rate-dependent model when compared to a strain level of 0.07 in the rate-independent model, Fig. 4-4c. The predicted slip shear increments on the conjugate slip system are identical thereafter in both the models.

4.1.2 Strain-Hardening Case

Here we consider the strain hardening model contained in equations (4.4, 4.5), with the listed material parameters. Recall that we are considering the case of a rather strong latent hardening with $q = 1.4$.

Figs. 4-5, 4-6 and 4-7 show the stress strain curves, the slip system activities, and the evolution of the crystal orientations obtained from the rate-independent model and the rate-dependent model during tension tests on single crystals with initial orientations [001], $[\bar{1}11]$, and $[\bar{2}36]$, respectively. Again, the results from the rate-independent model are almost indistinguishable from the rate-dependent model.

As before, there are eight slip systems activated in the [001] orientation. The slip activity on all the systems is equal, and the orientation is stable, Fig. 4-5. For the specimen in the $[\bar{1}11]$ orientation there are six activated slip systems, the slip activity on all the systems is equal, and the orientation is also stable, Fig. 4-6.

For the specimen initially oriented in the $[\bar{2}36]$ direction, as in the non-hardening case at first there is only slip system $A3 = (111)[\bar{1}01]$ which is activated, and during this single slip period the orientation of the tensile axis rotates on a great circle towards the slip direction $[\bar{1}01]$. However, the conjugate slip system $B5 = (11\bar{1})[011]$ does not get activated when the tensile axis reaches the $[001] - [\bar{1}11]$ boundary of the stereographic triangle, and the single slip regime *overshoots* it. The slip system B5 does not become active until an axial strain of ~ 0.12, which compares with an axial strain of ~ 0.07 for the non-hardening case. The physical reason for the overshoot is that since the latent hardening ratio q has been set to be greater than unity, slip on primary slip system $A3$ has hardened the latent slip system $B5$ much more than itself. Once the conjugate slip system does become active, there is an abrupt change in the direction of rotation of the tensile axis as seen in the Fig. 4-7c.

Since the orientation $[\bar{2}36]$ is not stable relative to the underlying lattice, there is macroscopic hardening due to a change in the orientation of the crystal lattice, and due to the hardening of the slip systems Fig. 4-7a.

The predictions of the rate-independent model are in excellent agreement with those of the rate-dependent model. Also, for the hardening case the predictions are in qualitative agreement with existing experimental observations of tension tests on f.c.c. materials which have been recently reviewed by Havner (1992, pp. 75). His summary findings are

paraphrased[2] below:

1. "In virgin crystals carefully oriented in high-symmetry (six- or eightfold) multiple-slip positions: (a) the loading axis is stable relative to the underlying lattice; (b) the deformation is ordinarily axisymmetric; and (c) the hardening of all systems (both active and latent) is very nearly equal.

2. In virgin crystals oriented for single slip either in tension or in compression: (a) the intersecting latent systems in general harden more than the active slip system; (b) significant overshooting is the norm in tests carried to that stage of axis rotation; and (c) typical deformation beyond the symmetry line is consistent with dominant single slip on the original system."

4.2 Simple Compression Simulation on Polycrystalline OFHC Copper

We have used an annealed OFHC copper in this study which has a reasonably random texture to start with. This texture is represented numerically by a set of "random" 400 grains as shown in Fig. 4-8. The hardening of the slip systems is represented by a simple model as presented in equation 4.4. The slip hardening parameters are taken as $h_o = 180$ MPa, $s_s = 148$ MPa $a = 2.25$, and $q = 1.4$ (Bornkhorst *et al*, 1992). For the rate dependent model, we take the reference shearing rate $\dot{\gamma}_0 = 0.001s^-1$ and $m = 0.012$. The simulations were performed in FEM package ABAQUS/Explicit.

4.2.1 FEM Model

An intial mesh of 343 ($=7^3$) cubic ABAQUS C3D8R elements was used in the calculations, Fig. 4-9b. As sketched in Fig. 4-9a., this mesh represents one-eight of a rectangular parellopiped specimen. Each element represents a single crystal, and is assingned an orientation randomly chosen from the set of initial 400 grain orientations whose pole figures were shown in Fig. 4-8. The macroscopic (1,2), (2,3) and (3,1)-planes of the meshed octant which are embedded in the model are constrained to remain plane. The top (1,2) plane was

[2]Havner also comments on the evolution of dislocation structures, but we do not go into that matter here.

contrained to remain plane and moved at a constant displacement rate.

The Deformed finite element meshes are shown in Fig. 4-10. Since the outside surfaces of the finit element mesh are unconstrained, a remarkable "oroange peel" effect is observed due to the differing orientations of the grains which intersect these free surfaces. This effect has also been observed in the experiment performed on OFHC copper (Bronkhorst, 1991). Fig. 4-11 and 4-12 show the stress-strain curves and the crystallographic texture at a compressive strain of 100% obtained from the rate-independent and the rate-dependent models. The results from both the models are almost identical. The stress-strain response and the texture are also in agreement with those experimently measured by Bronkhorst, Kalidindi and Anand (1992).

4.2.2 Taylor Model

A eight noded ABAQUS C3D8R element was used to perform the simple compression simulation on OFHC copper. The integration point was assigned the initial random 400 orientations and the macroscopic response at the integration point was obtained using the Taylor-type averaging procedure. The simulations were performed to a final true strain of -1.0.

Fig. 4-13 and 4-14 show the stress-strain response and the crystallographic texture at a strain on -1.0 obtained from the rate-independent and the rate-dependent model. The results from the rate-independent model are almost identical to that of the rate dependent model.

4.3 Conclusions

The predictions from the rate-independent model are in excellent agreement with those of the rate-dependent model in the rate-independent limit for both single crystal as well as polycrystalline f.c.c materials. The simple compression simulation has also demonstrated that the results from a Taylor-type and FEM rate-independent model are almost identical to that of a Taylor-type and FEM rate-dependent model in the rate-independent limit.

	α	$\mathbf{m}_o^\alpha$	$\mathbf{n}_o^\alpha$
1	A2	$\frac{1}{\sqrt{2}}$ $-\frac{1}{\sqrt{2}}$ 0	$\frac{1}{\sqrt{3}}$ $\frac{1}{\sqrt{3}}$ $\frac{1}{\sqrt{3}}$
2	A3	$-\frac{1}{\sqrt{2}}$ 0 $\frac{1}{\sqrt{2}}$	$\frac{1}{\sqrt{3}}$ $\frac{1}{\sqrt{3}}$ $\frac{1}{\sqrt{3}}$
3	A6	0 $\frac{1}{\sqrt{2}}$ $-\frac{1}{\sqrt{2}}$	$\frac{1}{\sqrt{3}}$ $\frac{1}{\sqrt{3}}$ $\frac{1}{\sqrt{3}}$
4	D4	$\frac{1}{\sqrt{2}}$ 0 $\frac{1}{\sqrt{2}}$	$-\frac{1}{\sqrt{3}}$ $\frac{1}{\sqrt{3}}$ $\frac{1}{\sqrt{3}}$
5	D1	$-\frac{1}{\sqrt{2}}$ $-\frac{1}{\sqrt{2}}$ 0	$-\frac{1}{\sqrt{3}}$ $\frac{1}{\sqrt{3}}$ $\frac{1}{\sqrt{3}}$
6	D6	0 $\frac{1}{\sqrt{2}}$ $-\frac{1}{\sqrt{2}}$	$-\frac{1}{\sqrt{3}}$ $\frac{1}{\sqrt{3}}$ $\frac{1}{\sqrt{3}}$
7	C3	$-\frac{1}{\sqrt{2}}$ 0 $\frac{1}{\sqrt{2}}$	$\frac{1}{\sqrt{3}}$ $-\frac{1}{\sqrt{3}}$ $\frac{1}{\sqrt{3}}$
8	C5	0 $-\frac{1}{\sqrt{2}}$ $-\frac{1}{\sqrt{2}}$	$\frac{1}{\sqrt{3}}$ $-\frac{1}{\sqrt{3}}$ $\frac{1}{\sqrt{3}}$
9	C1	$\frac{1}{\sqrt{2}}$ $\frac{1}{\sqrt{2}}$ 0	$\frac{1}{\sqrt{3}}$ $-\frac{1}{\sqrt{3}}$ $\frac{1}{\sqrt{3}}$
10	B2	$-\frac{1}{\sqrt{2}}$ $\frac{1}{\sqrt{2}}$ 0	$-\frac{1}{\sqrt{3}}$ $-\frac{1}{\sqrt{3}}$ $\frac{1}{\sqrt{3}}$
11	B4	$\frac{1}{\sqrt{2}}$ 0 $\frac{1}{\sqrt{2}}$	$-\frac{1}{\sqrt{3}}$ $-\frac{1}{\sqrt{3}}$ $\frac{1}{\sqrt{3}}$
12	B5	0 $-\frac{1}{\sqrt{2}}$ $-\frac{1}{\sqrt{2}}$	$-\frac{1}{\sqrt{3}}$ $-\frac{1}{\sqrt{3}}$ $\frac{1}{\sqrt{3}}$

Table 4.1: Components of $\mathbf{m}_0^\alpha$ and $\mathbf{n}_0^\alpha$ with respect to an orthonormal basis associated with the crystal lattice for FCC crystals

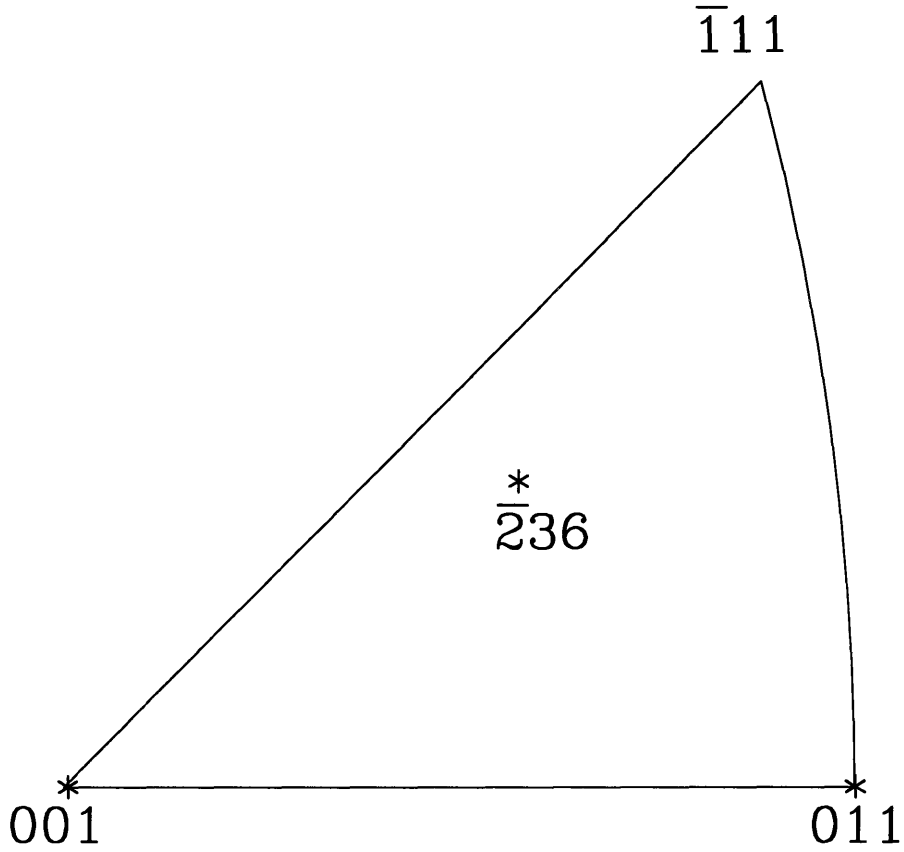

Figure 4-1: Primary orientation triangle in a [001] steregraphic projection. The symbol '*' denotes the initial orientations of the axes of the three tension tests considered.

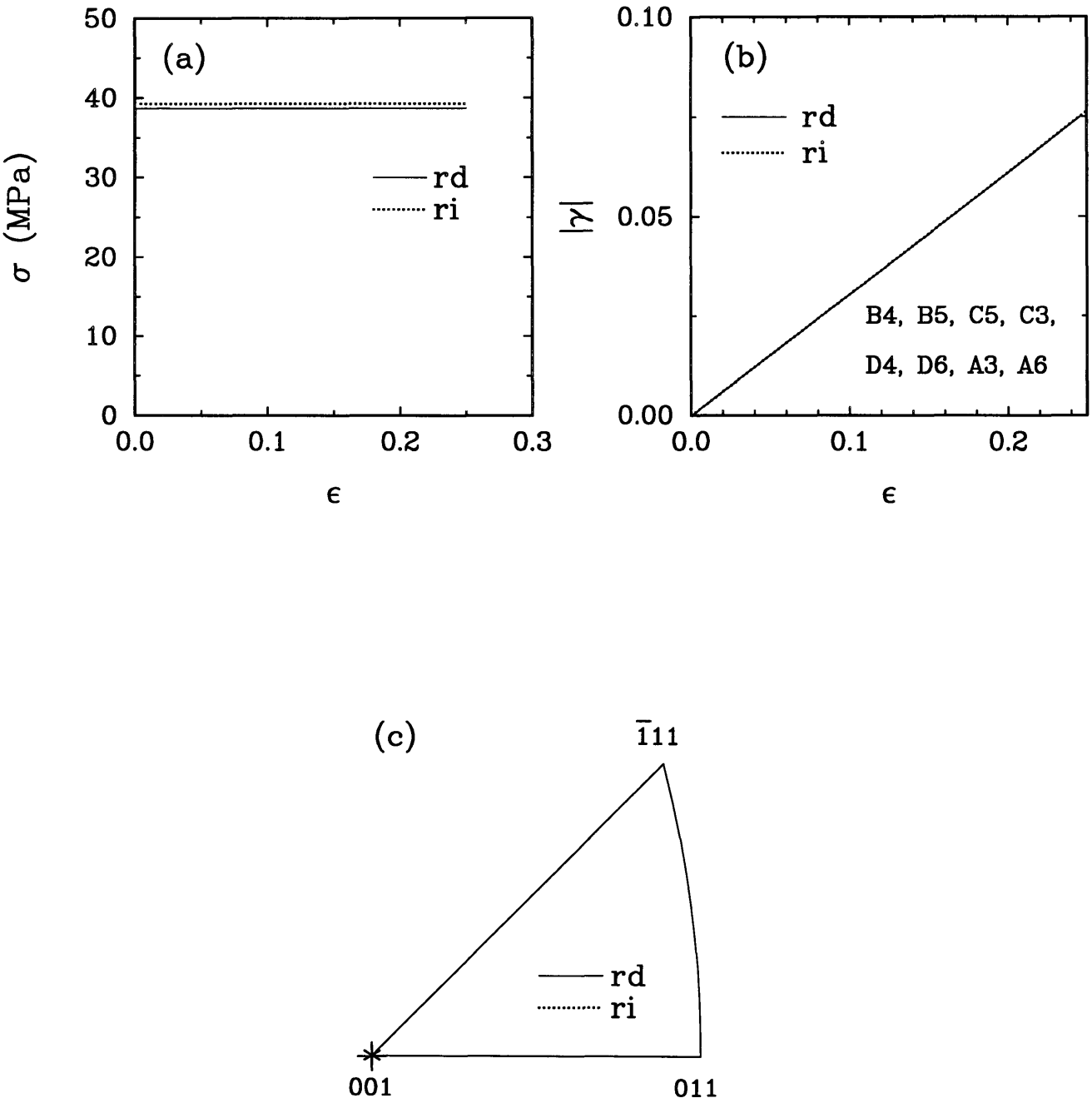

Figure 4-2: Comparison of the results from a rate-independent (ri) crystal plasticity model against those of a rate-dependent (rd) model for simple tension of a non-hardening crystal initially oriented in the [001] direction: (a) stress-strain curve; (b) slip shears; (c) inverse pole figure of the change in the orientation of the tensile axis ('*' denotes initial orientation and '+' denotes the final orientation).

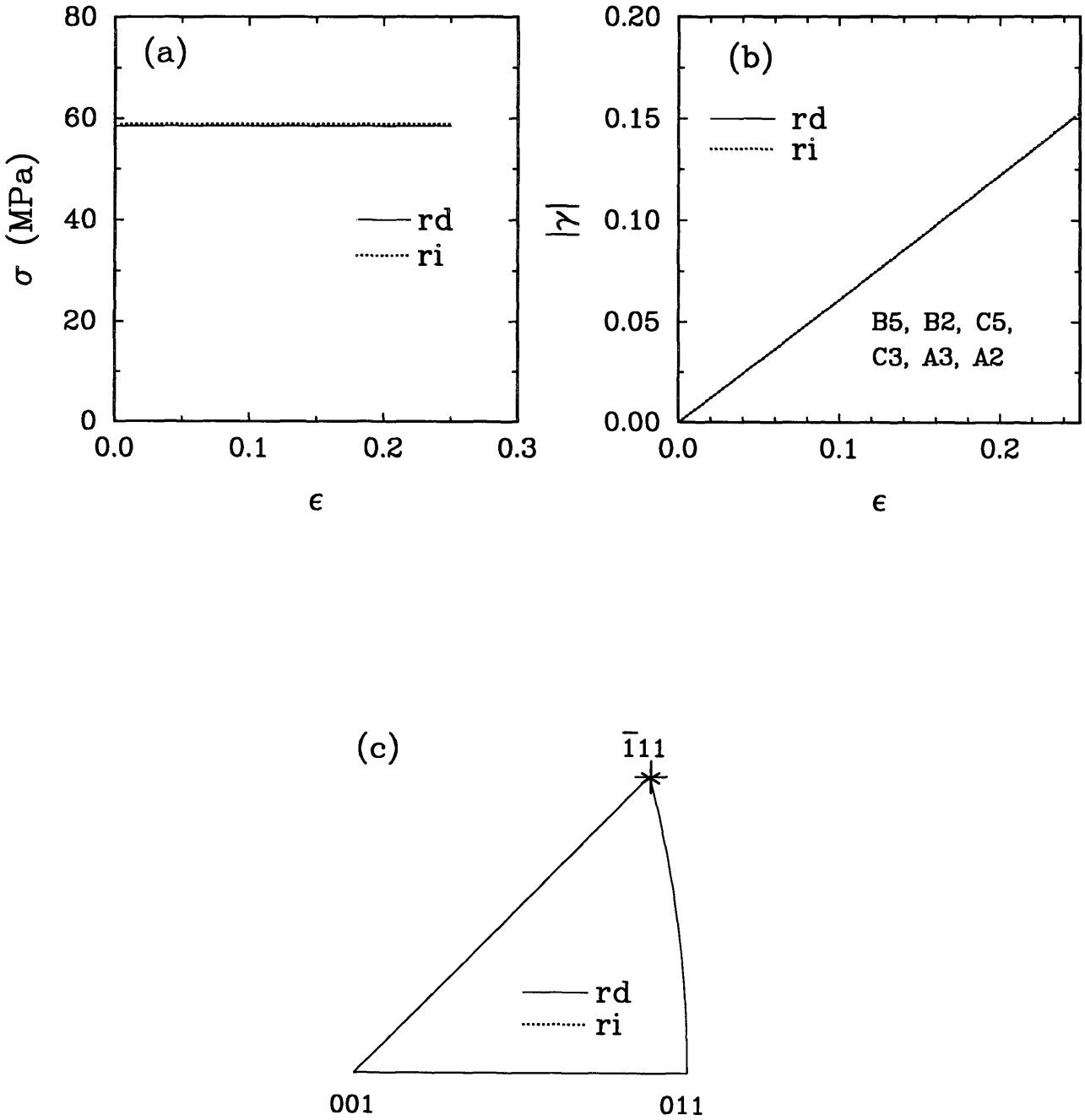

Figure 4-3: Comparison of the results from a rate-independent (ri) crystal plasticity model against those of a rate-dependent (rd) model for simple tension of a non-hardening crystal initially oriented in the [111] direction: (a) stress-strain curve; (b) slip shears; (c) inverse pole figure of the change in the orientation of the tensile axis ('*' denotes initial orientation and '+' denotes the final orientation).

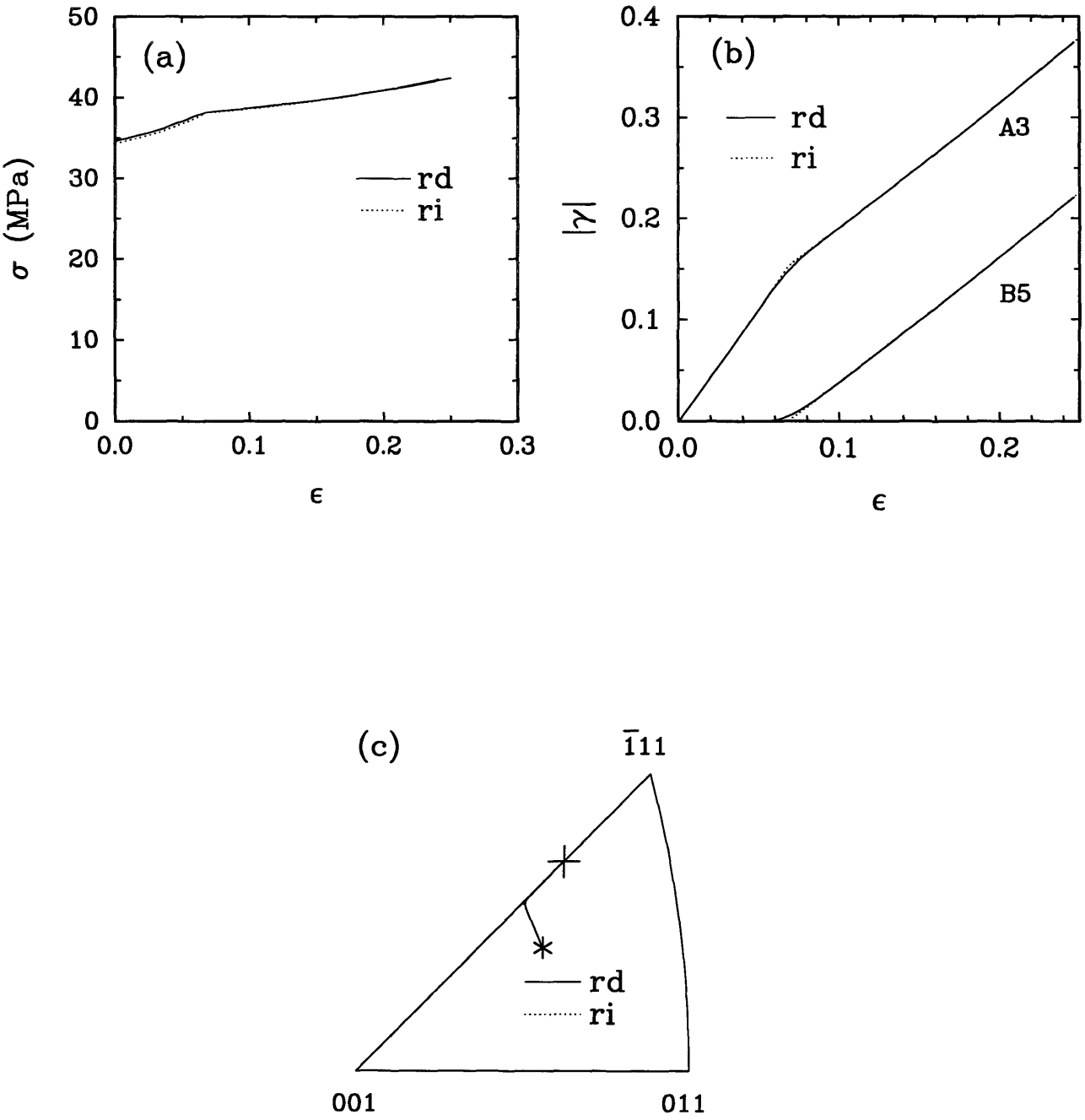

Figure 4-4: Comparison of the results from a rate-independent (ri) crystal plasticity model against those of a rate-dependent (rd) model for simple tension of a non-hardening crystal initially oriented in the [$\bar{2}36$] direction: (a) stress-strain curve; (b) slip shears; (c) inverse pole figure of the change in the orientation of the tensile axis ('*' denotes initial orientation and '+' denotes the final orientation).

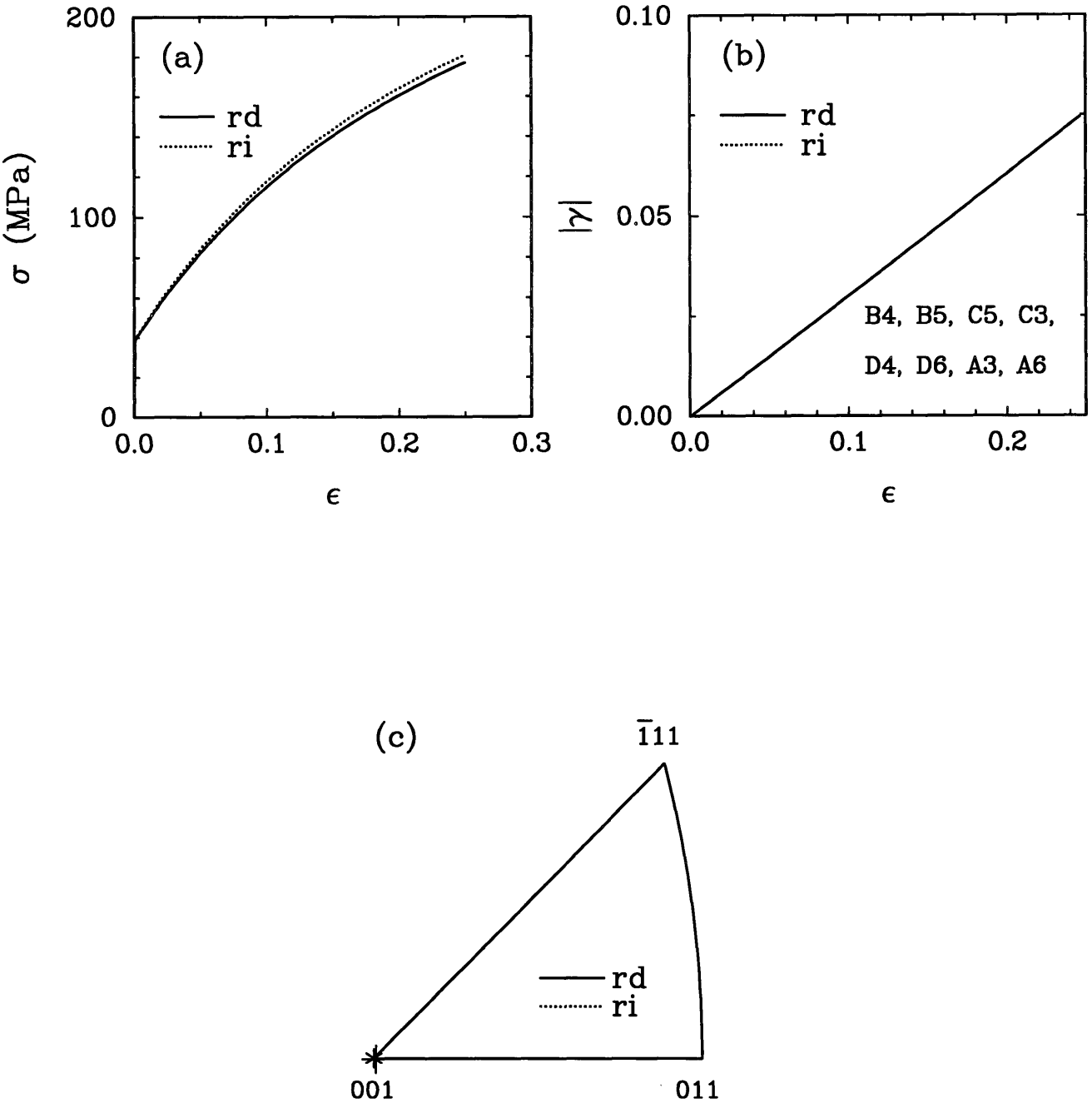

Figure 4-5: Comparison of the results from a rate-independent (ri) crystal plasticity model against those of a rate-dependent (rd) model for simple tension of a strain-hardening crystal initially oriented in the [001] direction: (a) stress-strain curve; (b) slip shears; (c) inverse pole figure of the change in the orientation of the tensile axis ('*' denotes initial orientation and '+' denotes the final orientation).

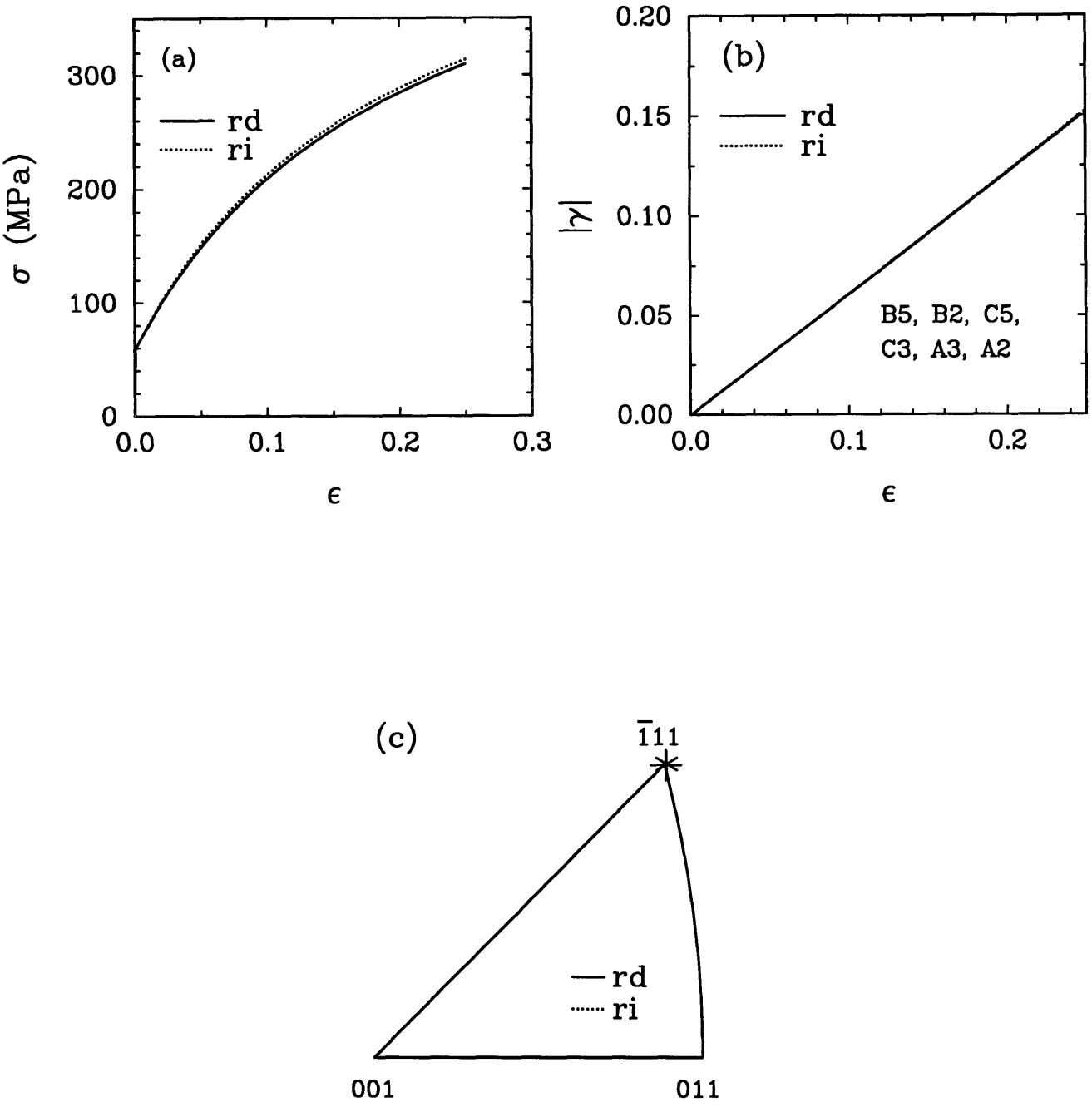

Figure 4-6: Comparison of the results from a rate-independent (ri) crystal plasticity model against those of a rate-dependent (rd) model for simple tension of a strain-hardening crystal initially oriented in the [111] direction: (a) stress-strain curve; (b) slip shears; (c) inverse pole figure of the change in the orientation of the tensile axis ('*' denotes initial orientation and '+' denotes the final orientation).

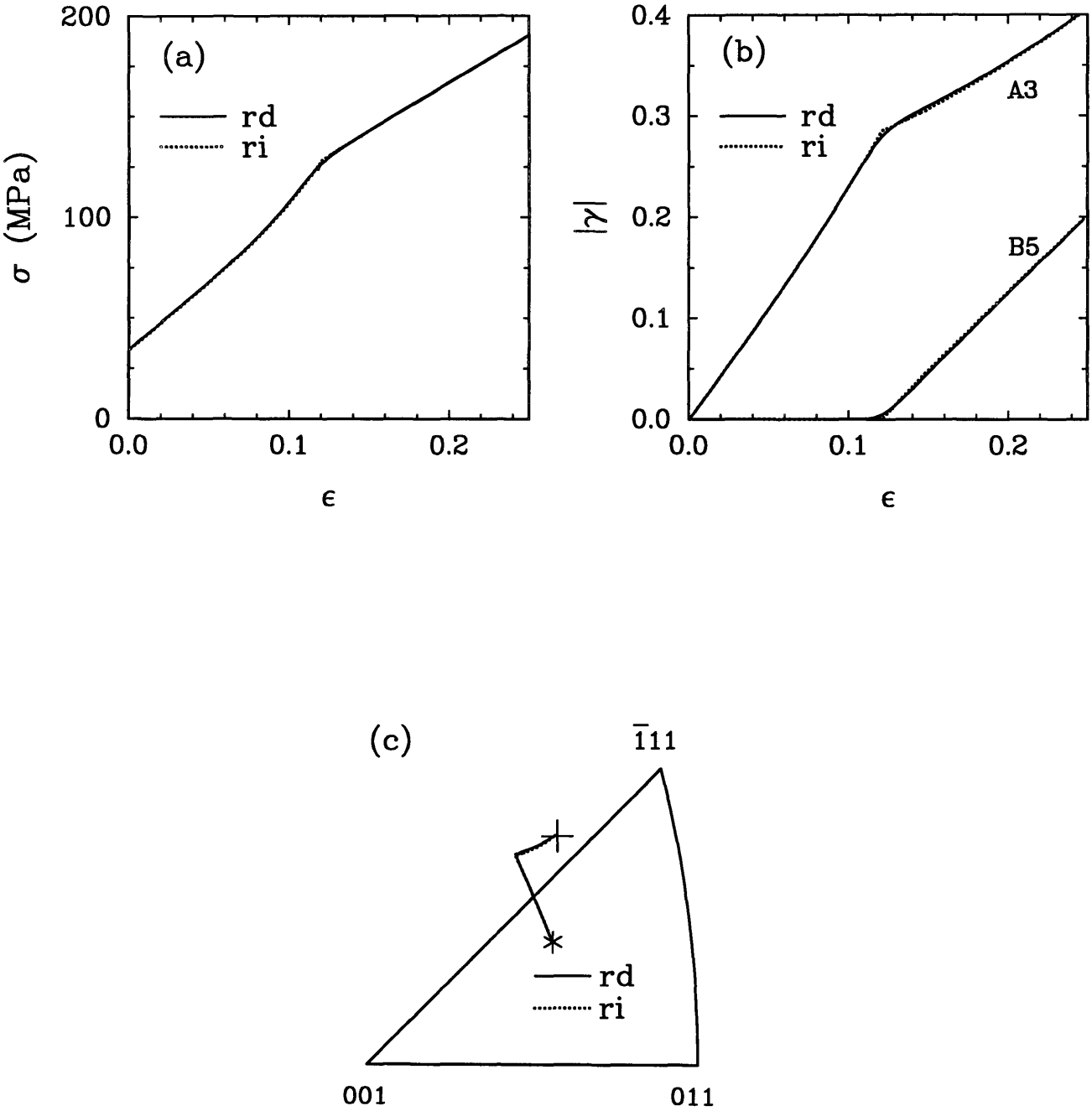

Figure 4-7: Comparison of the results from a rate-independent (ri) crystal plasticity model against those of a rate-dependent (rd) model for simple tension of a strain-hardening crystal initially oriented in the $[\bar{2}36]$ direction: (a) stress-strain curve; (b) slip shears; (c) inverse pole figure of the change in the orientation of the tensile axis ('*' denotes initial orientation and '+' denotes the final orientation).

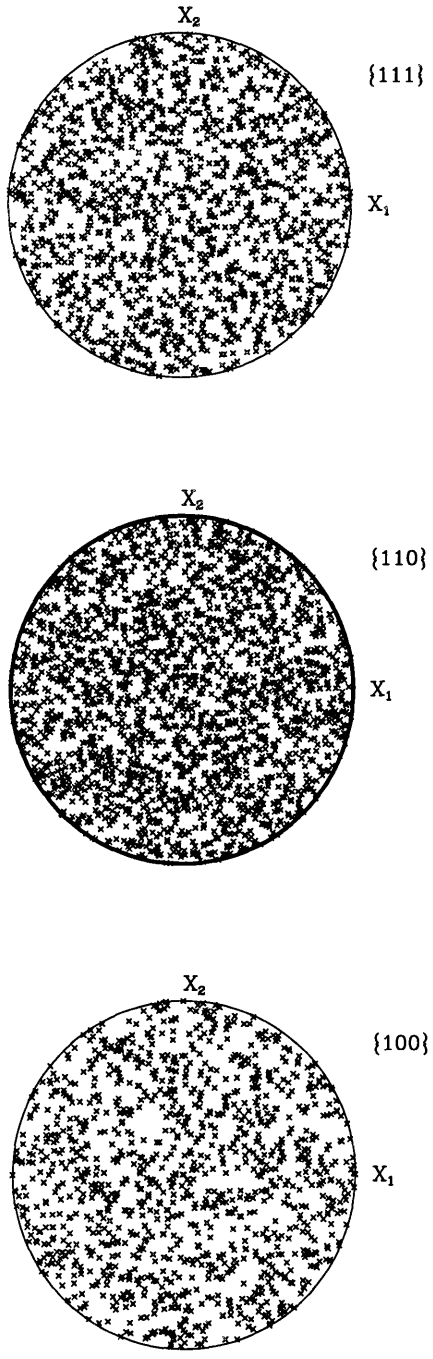

Figure 4-8: Initial Texture of OFHC Copper

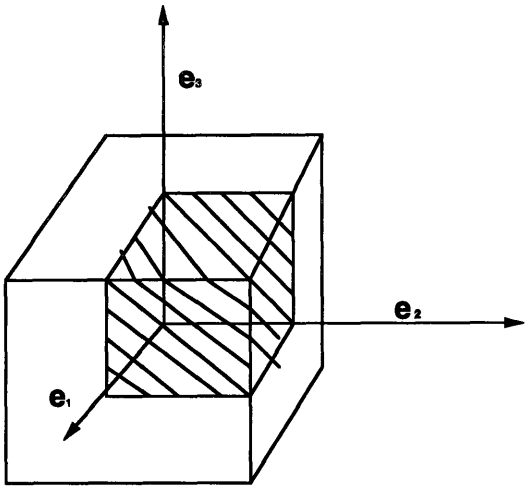

(a)

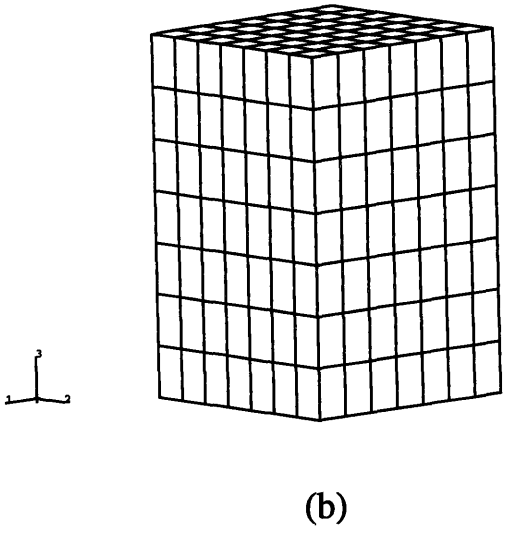

(b)

Figure 4-9: Initial mesh for simple compression simulation. (a) Octant of a cube. (b) Initial finite element mesh

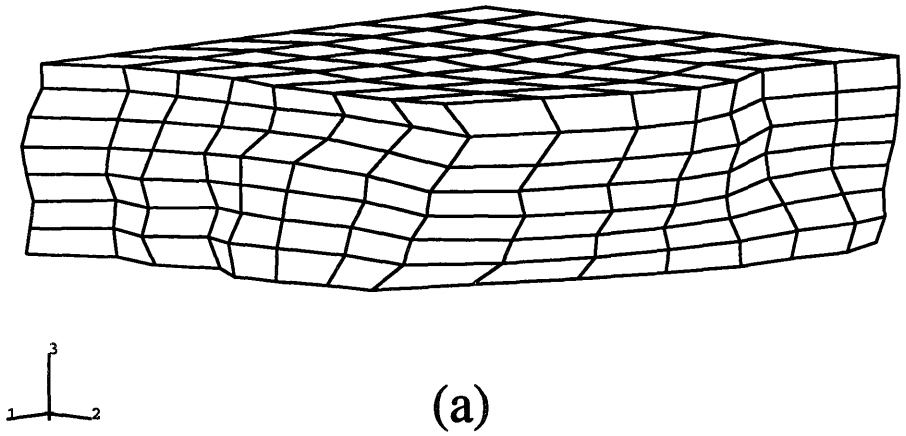

(a)

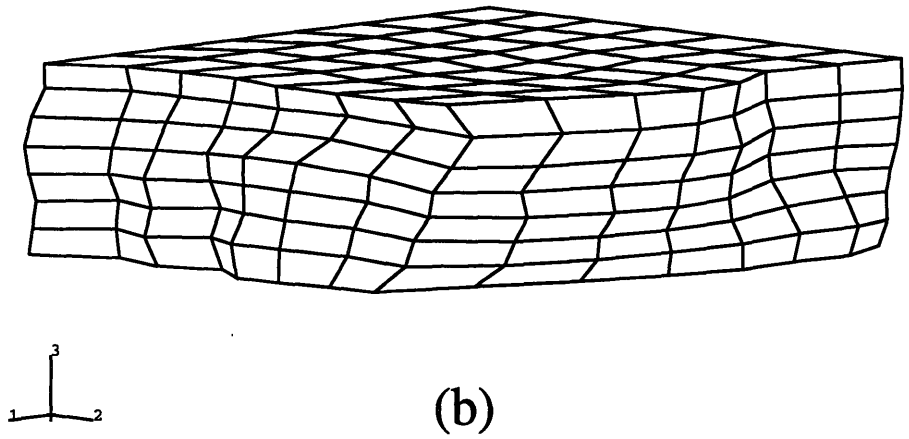

(b)

Figure 4-10: Deformed finite element mesh for simple compression simulation after a compressive strain of 100%. (a) rate dependent model. (b) rate-independent model

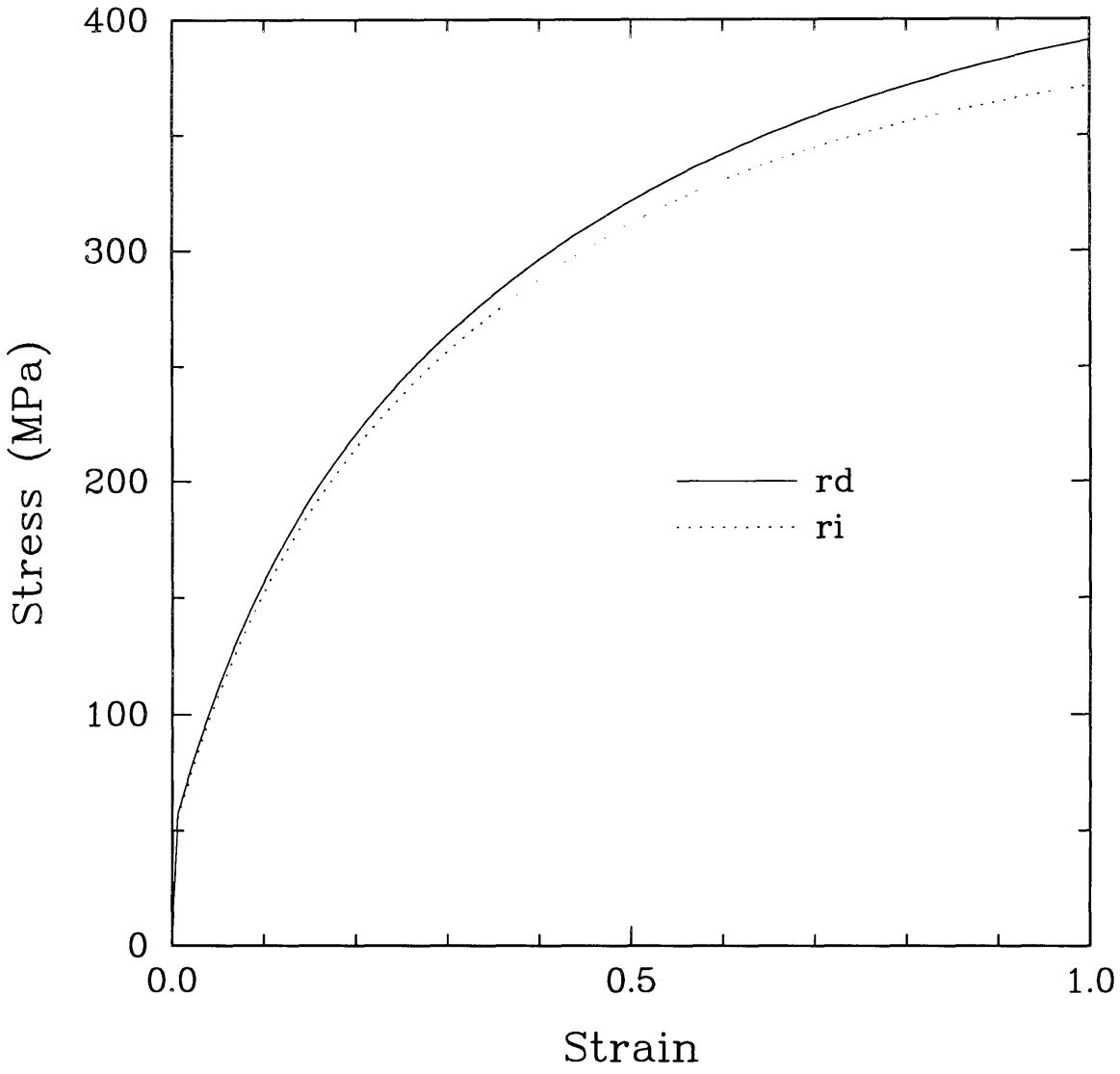

Figure 4-11: Comparison of the stress-strain response from a FEM rate-independent (ri) crystal plasticity model against those of a FEM rate-dependent (rd) model for simple compression of polycrystalline OFHC Copper

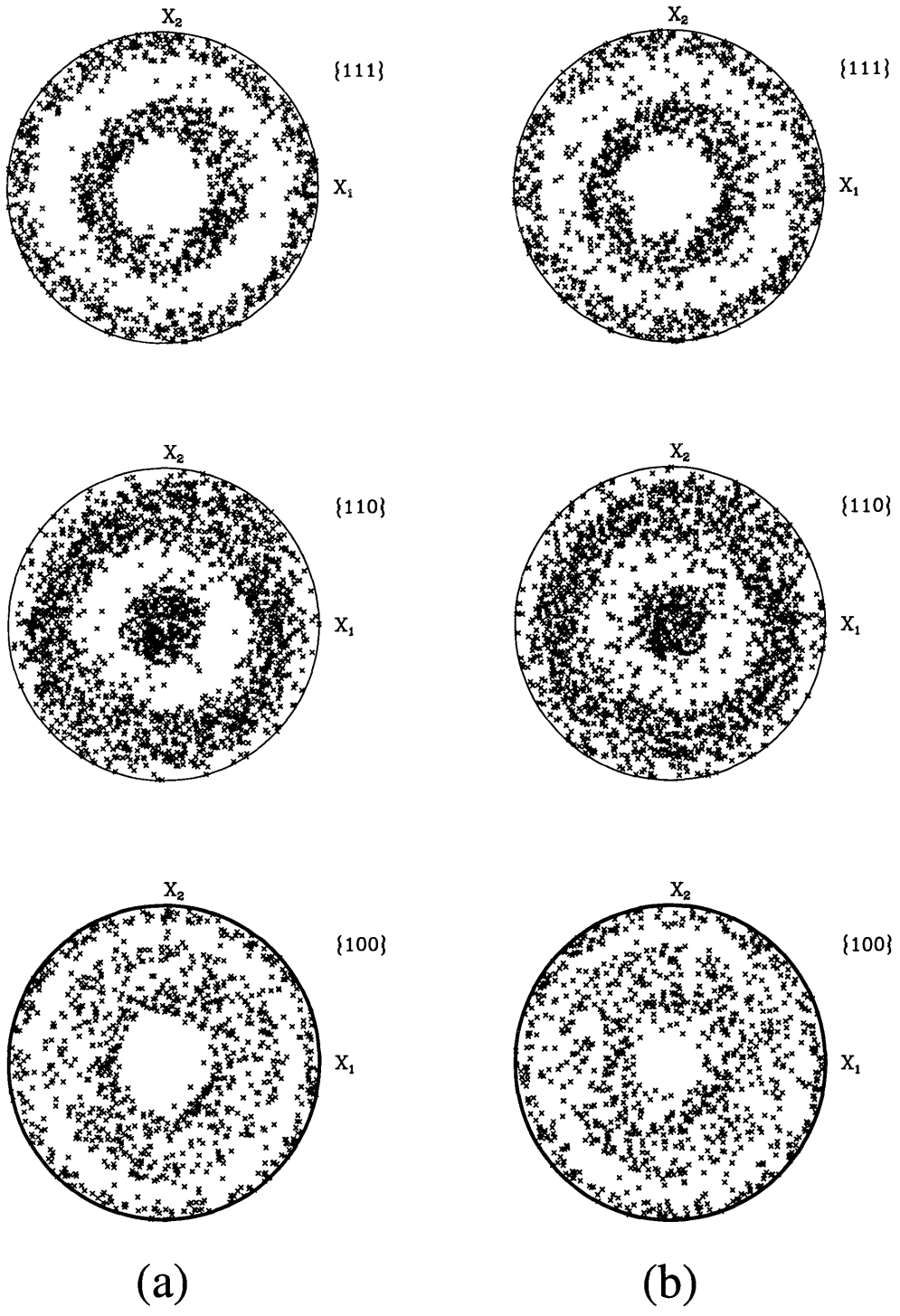

Figure 4-12: Comparison of the crystallographic texture at a strain of -1. for simple compression of polycrystalline OFHC Copper : (a) FEM rate-independent crystal plasticity model (b) FEM rate-dependent model

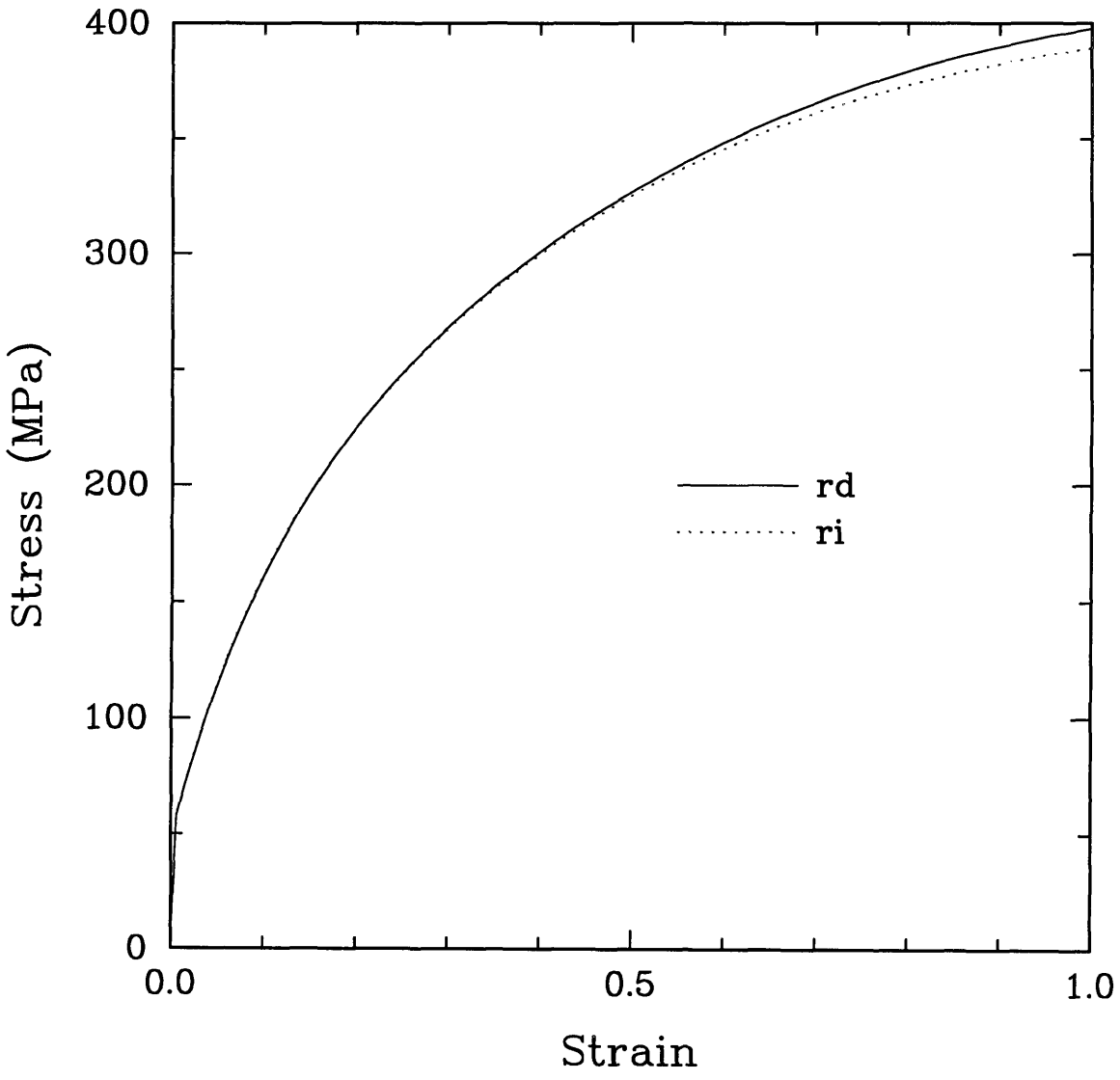

Figure 4-13: Comparison of the stress-strain response from a Taylor-type rate-independent (ri) crystal plasticity model against those of a Taylor-type rate-dependent (rd) model for simple compression of polycrystalline OFHC Copper

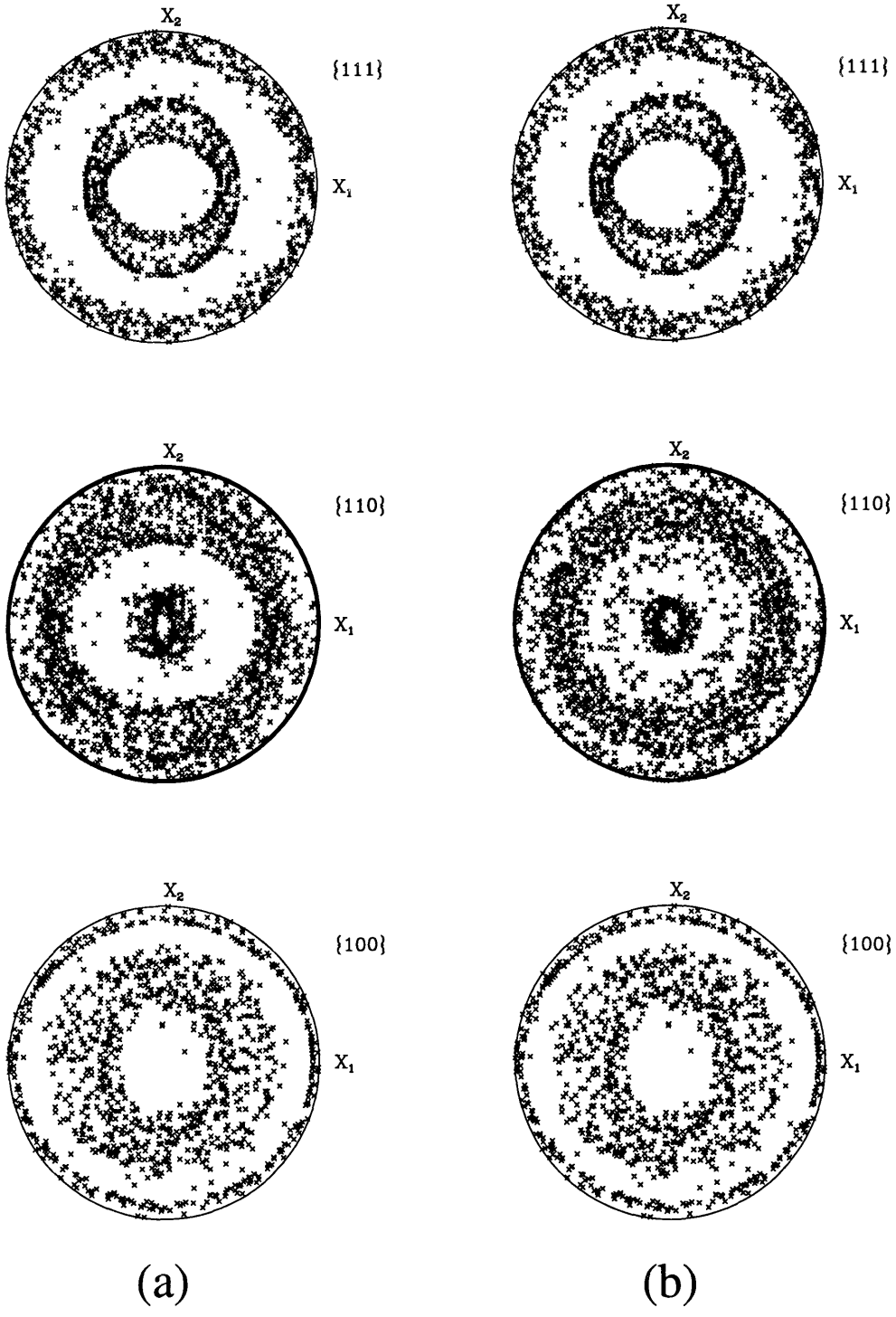

Figure 4-14: Comparison of the crystallographic texture at a strain of -1. for simple compression of polycrystalline OFHC Copper : (a) Taylor-type rate-independent crystal plasticity model (b) Taylor-type rate-dependent model

References

1923 Taylor, G. I., and Elam, C. F.,"The Distortion Of An Aluminum Crystal During A Tensile Test," *Proceedings of the Royal Society*, **A 102**, pp. 643 – 667.

1925 Taylor, G. I., and Elam, C. F.,"The Plastic Extennsion And Fracture Of Aluminum Single Crystals," *Proceedings of the Royal Society*, **A 108**, pp. 28 – 51.

1938a Taylor, G. I., "Plastic Strain In Metals," *Journal of The Institute of Metals*, **62**, pp. 307 - 324.

1938b Taylor, G. I.,"Analysis Of Plastic Strain In A Cubic Crystal," *Stephen Timoshenko 60th Anniversary Volume*, McMillan Co., New York, pp. 218 – 224.

1951a Bishop, J. F. W., and Hill, R.,"A Theory Of The Plastic Distortion Of A Polycrystalline Aggregate Under Combined Stresses," *Philosophical Magazine*, **Ser. 7, 42**, pp. 414 – 427.

1951b Bishop, J. F. W., and Hill, R.,"A Theoretical Derivation Of The Plastic Properties Of Polycrystalline Face Centered Metal," *Philosophical Magazine*, **Ser. 7, 42**, pp. 1298 – 1307..

1965 Mandel, J., "Generalisation de la theorie de plasticite De W.T. Koiter," *International Journal of Solids and Structures*, **1**, pp. 273 – 295.

1966 Hill, R.,"Generalized Constitutive Relations For Incremental Deformation of Metal Crystals by Mutislip," *Journal of The Mechanics and Physics of Solids*, **14**, pp. 95 – 102.

1969 Chin, G. Y., and Mammel,"Generalization and Equivalence of The Minimum Work (Taylor) and Maximum Work(Bishop-Hill) Principles for Crystal Plasticity," *Transaction Of The Metallurgical Society Of AIME*, **245**, pp. 1211 – 1214.

1971 Rice, J.R.,"Inelastic Constitutive Relations for Solids: An Internal Variable Theory and its Application to Metal Plasticity," *Journal of The Mechanics and Physics of Solids*, **19**, pp. 433 – 455.

1971 Simmons, G. and Wang, H.,*Single Crystal Elastic Constants and Calculated Aggregate Properties*, The M.I.T Press, Cambridge.

1972 Hill, R., and Rice, J.R., "Constitutive Analysis of Elastic-Plastic Crystals at Arbitrary Strain," *Journal of The Mechanics and Physics of Solids*, **20**, pp. 401 – 413.

1974 Mandel, J.,"Thermodynamics and Plasticity," in Delgado Domingos, J. J., Nina, M. N. R., and Whitelaw, J. H. (eds.) *Proceedings of The International Symposium on Foundations of Continuum Thermodynamics*, McMillan, London, pp. 283 – 311.

1976 Hutchinson, J.W., "Bounds and Self-Consistent Estimates for Creep of Polycyrtalline Materials," *Proceedings of the Royal Society of London A*, **348**, pp. 101 – 127.

1977 Asaro, R.J. and Rice, J.R., "Strain Localization in Ductile Single Crystals," *Journal of The Mechanics and Physics of Solids*, **25**, pp. 309 – 338.

1981 Gurtin, M.E., *An Introduction to Continuum Mechanics*, Academic Press, New York.

1982 Peirce, D., Asaro, R. J., and Needleman, A., "An Analysis Of Nonuniform And Localized Deformation In Ductile Single Crystals," *Acta Metallurgica*, **30**, pp. 1087 – 1119.

1983a Asaro, R.J. , "Micromechanics of Crystals and Polycrystals," *Advances in Applied Mechanics* ., **23**, pp. 1 – 115.

1983b Asaro, R.J., Crystal Plasticity. *ASME Journal of Applied Mechanics.*, **50**, pp. 921 – 934.

1983 Golub, G. H., and Van Loan, C. F., *Matrix Computations*, The Johns Hopkins University Press, Balitomre, Maryland.

1985 Asaro, R.J. and Needleman, A., "Texture Development and Strain Hardening in Rate Dependent Polycrystals," *Acta Metallurgica.*, **33**, pp. 923 – 953.

1986 Press, W. H., Flannery, B. P., Teukolsky, and Vetterling, W. T., *Numerical Recipes. The Art of Scientific Computing*, Cambrige University Press, Cambridge.

1988 Strang, G., *Linear Algebra nad Its Applications*, Harcourt Brace Jovanovich College Publishers, Fort Worth.

1989 Brown, S., Kim, K. and Anand, L., "An Internal Variable Constitutive Model for Hot Working of Metals," *Journal of The Mechanics and Physics of Solids*, **5**, pp. 95 – 130.

1989 Strang, G.,*Linear Algebra and It's Applications*, Harcourt Brace Jovanovich, publishers.

1989 Press, W.H., Flannery, B.P., Teukolsky, S.A. and Vetterling, W.T., *Numerical Recipes : The Art of Scientific Computing*, Cambridge University Press.

1989 Golub, G.H. and Van Loan, C.F., *Matrix Computations*, Johns Hopkins University Press.

1990 Weber, G., Lush, A. M., Zavaliangos, A., and Anand, L.,"An Objective Time-Integration Procedure For Isotropic Rate-Independent and Rate-Dependent Elastic-Plastic Constitutive Equations," *International Journal of Plasticity*, **6**, pp. 701 – 744.

1991 Wu, Tien-Yue, Bassani, J. L. and Laird, C., "Latent Hardening in Single Crystals I. Theory and experiments," *Proceedings of the Royal Society of London A.*, **435**, pp. 1 – 19.

1991 Bassani, J. L. and Wu, Tien-Yue, "Latent Hardening in Single Crystals II. Analytical characterisation and predictions," *Proceedings of the Royal Society of London A.*, **435**, pp. 21 – 41.

1991 Bronkhorst, C., "Plastic Deformation and Crystallographic Texture Evolution in Face-Centered Cubic Metals," Ph.D. thesis, MIT.

1992 Havner, K. S., *Finite Deformation of Crystalline Solids*, Cambridge University Press.

1992 Kalidindi, S. R., "Polycrystal Plasticity: Constitutive Modeling And Deformation Processing," Ph.D. thesis, MIT.

1992 Kalidindi, S.R., Bronkhorst, C.A., and Anand, L., "Crystallographic Texture Evolution During Bulk Deformation Processing of FCC Metals," *Journal of The Mechanics and Physics of Solids*, **40**, pp. 537 – 569.

1992 Bronkhorst, C.A., Kalidindi, S.R., and Anand, L., "Polycrystal Plasticity and the Evolution of Crystallographic Texture in Face-Centered Cubic Metals," *Philosophical Transactions of The Royal Society London A*, **341**, pp. 443 – 477.

1992 Kalidindi, S. R., and Anand, L.,"Large Deformation Simple Compression of a Copper Single Crystal," *Metallurgical Transactions*, **24A**, pp. 989 – 992.

1993 Hosford, W.F., *The Mechanics Of Crystals and Textured Polycrystals*, Oxford University Press.

1994 Anand,L., and Kalidindi, S. R.,"The Process Of Shear Band Formation In Plane Strain Compression Of FCC Metals: Effects Of Crystallographic Texture," *Mechanicsof Materials*, accepted for publication.

1994 Bassani, J. L.,"Plastic Flow of Crystals," *Advances in Applied Mechanics.*, **30**, pp. 191 - 258.

1994 ABAQUS *Reference Manuals.*, Hibbit, Karlson and Sorenson Inc., Pawtucket, R.I.